

# Recent results from COHERENT's inelastic neutrino-nucleus scattering detectors

Samuel Hedges

Interplay of Nuclear, Neutrino and BSM Physics at Low-Energies

April 18<sup>th</sup>, 2023



# Outline

- The COHERENT collaboration and neutrinos at the SNS
- Neutrino-induced neutron measurement on  $^{\text{nat}}\text{Pb}$
- Inclusive neutrino-nucleus scattering on  $^{127}\text{I}$
- COHERENT's future inelastic neutrino-nucleus measurements

# The COHERENT Collaboration & Neutrinos at the SNS

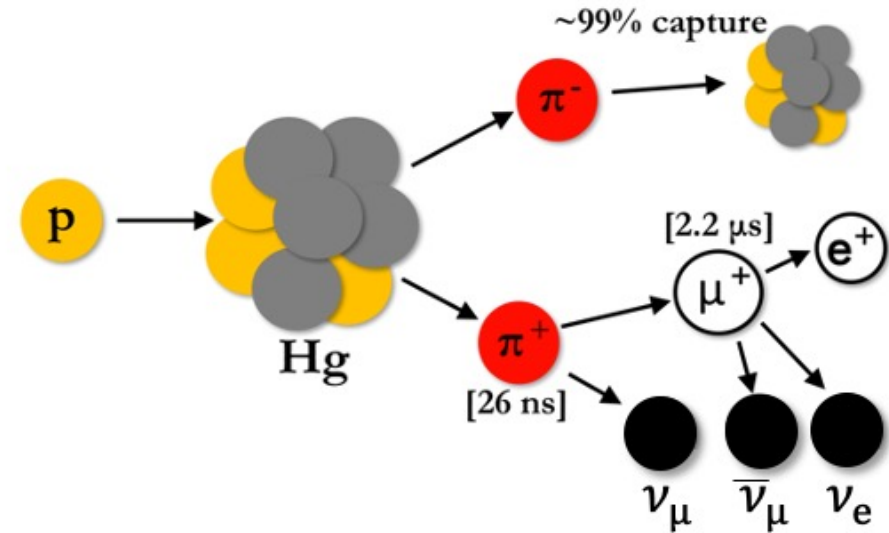
# The COHERENT Collaboration

- ~80 members, 20 institutions
- Formed to observe CEvNS, study physics in multiple targets, including  $N^2$  scaling of cross section
- Use neutrinos produced by the Spallation Neutron Source (SNS) at Oak Ridge National Laboratory (ORNL)
- Intense flux of low-energy pulsed neutrinos useful for studying inelastic neutrino-nucleus interactions as well

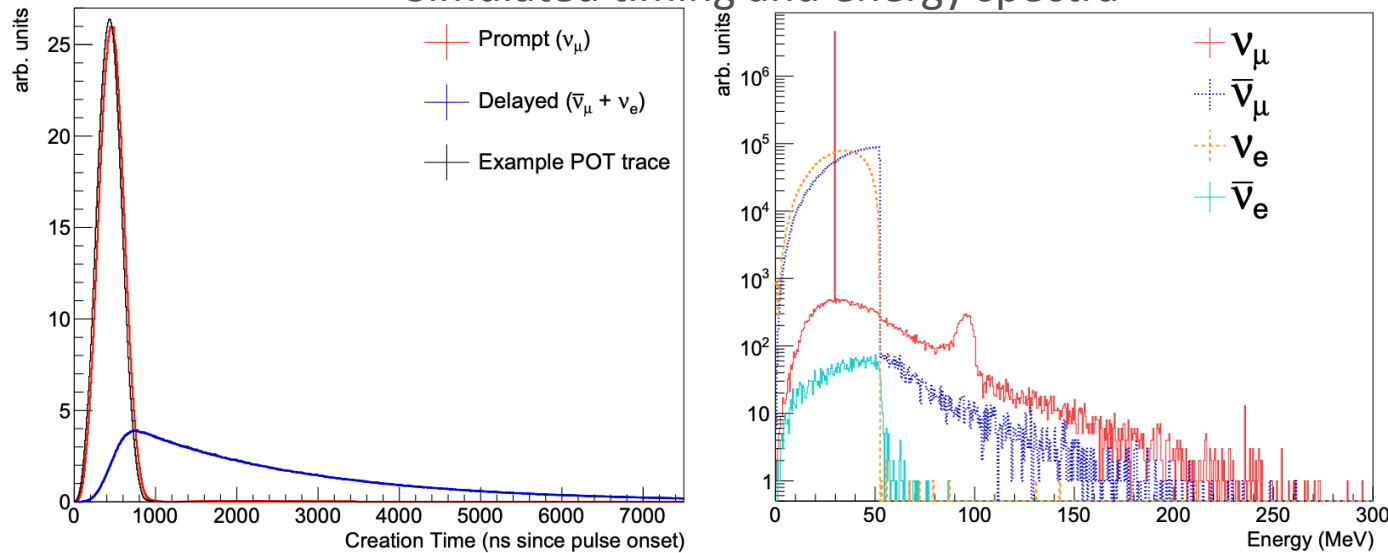


# Neutrinos at the SNS

- 1 GeV protons strike Hg target at the SNS at 60Hz
  - 350ns FWHM of proton pulse
- Produces  $\pi^-$  and  $\pi^+$  (and neutrons)
  - Neutrons are a background for our detectors, we refer to them as beam-related neutrons (**BRNs**)
- $\pi^+$  decay in  $\sim 26$ ns, leading to prompt  $\nu_\mu$  ( $\sim 30$  MeV) and  $\mu^+$
- $\mu^+$  decay with lifetime of  $2.2\mu\text{s}$ , producing delayed  $\nu_e$  and  $\bar{\nu}_\mu$  ( $< 53$  MeV)
  - $\nu_\mu$  roughly in time with beam,  $\nu_e$  and  $\bar{\nu}_\mu$  largely free from beam-related backgrounds



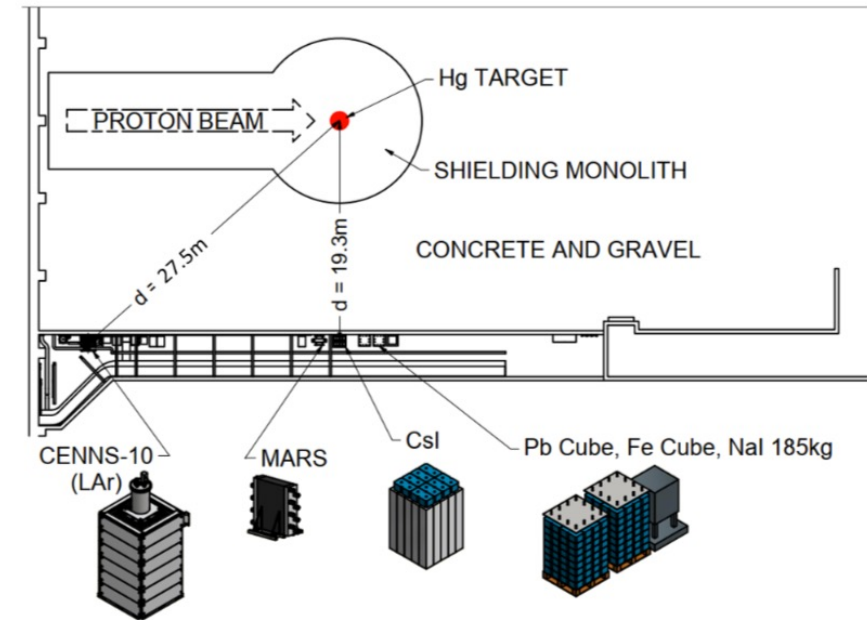
Simulated timing and energy spectra



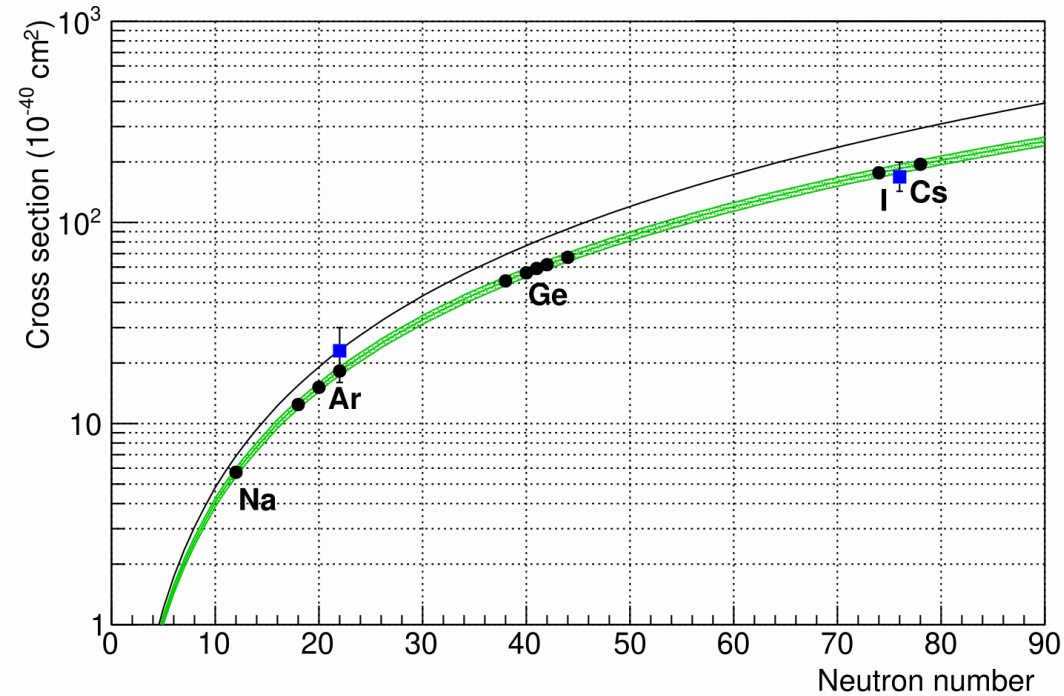
[D. Akimov, et al., arXiv:2109.11049 (2021)]

# Neutrino Alley

- COHERENT's detectors in "Neutrino Alley" at the SNS
  - 25m long hallway, 20-30m from target
  - Not designed for neutrino detectors
  - Concrete and gravel reduce beam neutrons
- Dedicated detectors for measuring neutrons



# COHERENT's CEvNS Detectors



Target	Technology	Mass (kg)	Threshold ( $\text{keV}_{nr}$ )	Date
CsI	CsI[Na] scintillator	14.6	6.5	6/2015
Ar	Single-phase liquid argon	24	20	12/2016
Na	NaI[Tl] scintillator array	185/2,425	13	2016/2022
Ge	p-type point contact Ge	16	3	2022

# Existing Low-Energy Neutrino-Nucleus Measurements

List of <300 MeV neutrino-nucleus measurements with terrestrial sources

Isotope	Reaction Channel	Source	Experiment	Measurement ( $10^{-42} \text{ cm}^2$ )	Theory ( $10^{-42} \text{ cm}^2$ )
$^2\text{H}$	$^2\text{H}(\nu_e, e^-)pp$	Stopped $\pi/\mu$	LAMPF	$52 \pm 18(\text{tot})$	54 (IA) (Tatara <i>et al.</i> , 1990)
$^{12}\text{C}$	$^{12}\text{C}(\nu_e, e^-)^{12}\text{N}_{\text{g.s.}}$	Stopped $\pi/\mu$	KARMEN	$9.1 \pm 0.5(\text{stat}) \pm 0.8(\text{sys})$	9.4 [Multipole](Donnelly and Peccei, 1979)
		Stopped $\pi/\mu$	E225	$10.5 \pm 1.0(\text{stat}) \pm 1.0(\text{sys})$	9.2 [EPT] (Fukugita <i>et al.</i> , 1988).
		Stopped $\pi/\mu$	LSND	$8.9 \pm 0.3(\text{stat}) \pm 0.9(\text{sys})$	8.9 [CRPA] (Kolbe <i>et al.</i> , 1999b)
	$^{12}\text{C}(\nu_e, e^-)^{12}\text{N}^*$	Stopped $\pi/\mu$	KARMEN	$5.1 \pm 0.6(\text{stat}) \pm 0.5(\text{sys})$	5.4-5.6 [CRPA] (Kolbe <i>et al.</i> , 1999b)
		Stopped $\pi/\mu$	E225	$3.6 \pm 2.0(\text{tot})$	4.1 [Shell] (Hayes and S, 2000)
		Stopped $\pi/\mu$	LSND	$4.3 \pm 0.4(\text{stat}) \pm 0.6(\text{sys})$	
	$^{12}\text{C}(\nu_\mu, \nu_\mu)^{12}\text{C}^*$	Stopped $\pi/\mu$	KARMEN	$3.2 \pm 0.5(\text{stat}) \pm 0.4(\text{sys})$	2.8 [CRPA] (Kolbe <i>et al.</i> , 1999b)
	$^{12}\text{C}(\nu, \nu)^{12}\text{C}^*$	Stopped $\pi/\mu$	KARMEN	$10.5 \pm 1.0(\text{stat}) \pm 0.9(\text{sys})$	10.5 [CRPA] (Kolbe <i>et al.</i> , 1999b)
	$^{12}\text{C}(\nu_\mu, \mu^-)X$	Decay in Flight	LSND	$1060 \pm 30(\text{stat}) \pm 180(\text{sys})$	1750-1780 [CRPA] (Kolbe <i>et al.</i> , 1999b)
					1380 [Shell] (Hayes and S, 2000) 1115 [Green's Function] (Meucci <i>et al.</i> , 2004)
$^{12}\text{C}(\nu_\mu, \mu^-)^{12}\text{N}_{\text{g.s.}}$	Decay in Flight	LSND	$56 \pm 8(\text{stat}) \pm 10(\text{sys})$	68-73 [CRPA] (Kolbe <i>et al.</i> , 1999b) 56 [Shell] (Hayes and S, 2000)	
$^{56}\text{Fe}$	$^{56}\text{Fe}(\nu_e, e^-)^{56}\text{Co}$	Stopped $\pi/\mu$	KARMEN	$256 \pm 108(\text{stat}) \pm 43(\text{sys})$	264 [Shell] (Kolbe <i>et al.</i> , 1999a)
$^{71}\text{Ga}$	$^{71}\text{Ga}(\nu_e, e^-)^{71}\text{Ge}$	$^{51}\text{Cr}$ source	GALLEX, ave.	$0.0054 \pm 0.0009(\text{tot})$	0.0058 [Shell] (Haxton, 1998)
		$^{51}\text{Cr}$	SAGE	$0.0055 \pm 0.0007(\text{tot})$	
		$^{37}\text{Ar}$ source	SAGE	$0.0055 \pm 0.0006(\text{tot})$	0.0070 [Shell] (Bahcall, 1997)
$^{127}\text{I}$	$^{127}\text{I}(\nu_e, e^-)^{127}\text{Xe}$	Stopped $\pi/\mu$	LSND	$284 \pm 91(\text{stat}) \pm 25(\text{sys})$	210-310 [Quasi-particle] (Engel <i>et al.</i> , 1994)

[J. A. Formaggio & G. P. Zeller, Rev. Mod. Phys **84** (2012)]



# COHERENT's Inelastic Detectors



= existing measurements for low-energy (<300 MeV) neutrinos from terrestrial sources



= COHERENT's current & planned detectors

57 La Lanthanum 138.90547	58 Ce Cerium 140.12708	59 Pr Praseodymium 140.90768	60 Nd Neodymium 144.242	61 Pm Promethium (145)	62 Sm Samarium 150.36	63 Eu Europium 151.964	64 Gd Gadolinium 157.25	65 Tb Terbium 158.92535	66 Dy Dysprosium 162.500	67 Ho Holmium 164.93033	68 Er Erbium 167.259	69 Tm Thulium 168.93422	70 Yb Ytterbium 173.054	71 Lu Lutetium 174.967
89 Ac Actinium (227)	90 Th Thorium 232.0377	91 Pa Protactinium 231.03688	92 U Uranium 238.02891	93 Np Neptunium (237)	94 Pu Plutonium (244)	95 Am Americium (243)	96 Cm Curium (247)	97 Bk Berkelium (247)	98 Cf Californium (251)	99 Es Einsteinium (252)	100 Fm Fermium (257)	101 Md Mendelevium (258)	102 No Nobelium (259)	103 Lr Lawrencium (260)

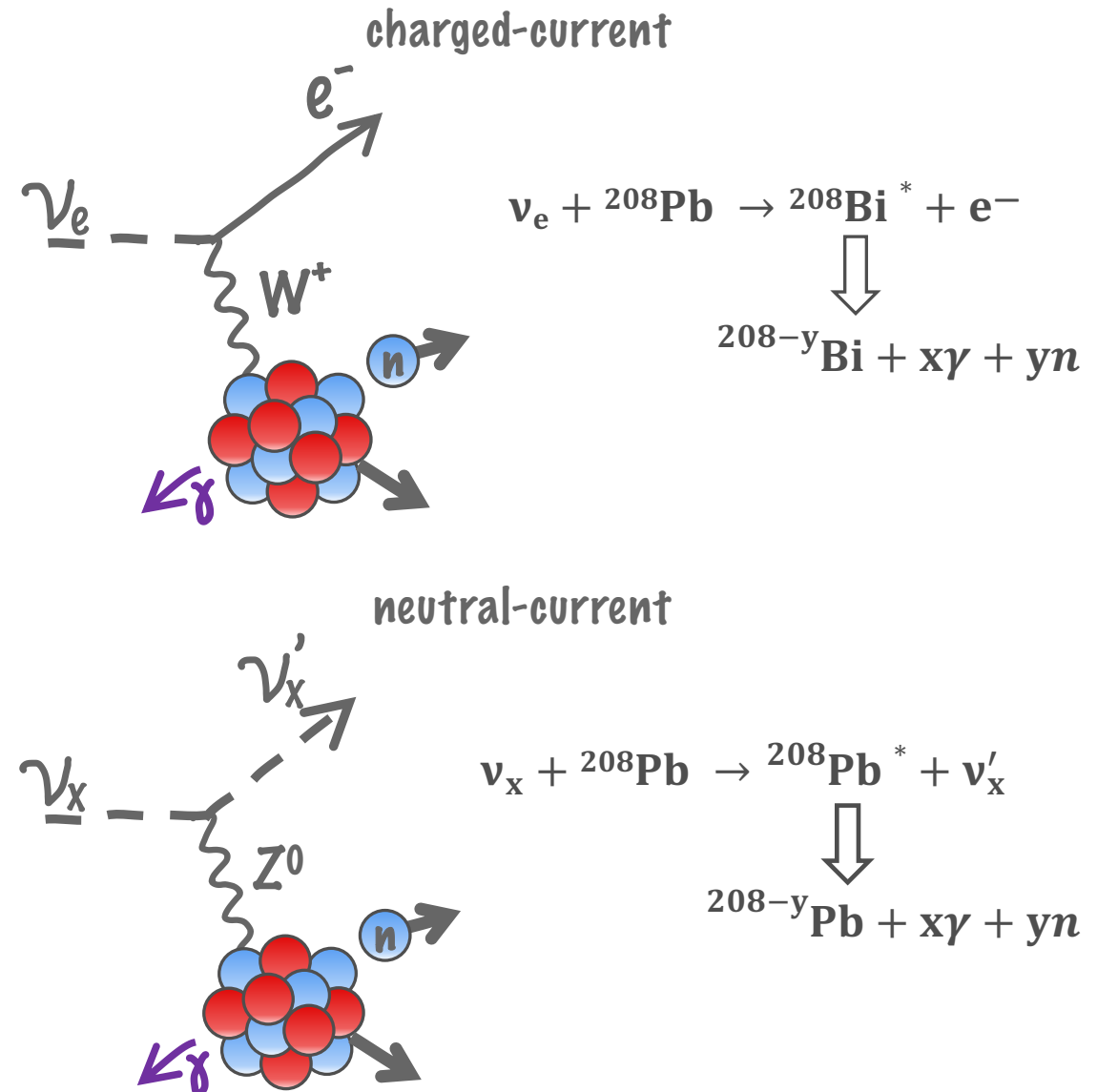
Name	Target	Channel	Deployment Date
Lead Neutrino Cube	Lead	$Pb(\nu_e, e^- + xn)$	1/2016
Iron Neutrino Cube	Iron	$Fe(\nu_e, e^- + xn)$	2/2017
NaI $\nu$ E (COH-NaI-185)	$^{127}\text{I}$	$^{127}\text{I}(\nu_e, e^- + x)$	6/2016
CENNS-10 (COH-Ar-10)	Argon	$Ar(\nu_e, e^- + x)$	2017
$\nu$ Thor	Thorium	$Th(\nu_e, e^- + x)$	2022
CENNS-750 (COH-Ar-750)	Argon	$Ar(\nu_e, e^- + x)$	future
D <sub>2</sub> O	$^2\text{H}/\text{O}$	$^2\text{H}/\text{O}(\nu_e, e^- + x)$	future

Results presented today!

# Neutrino-induced neutron measurement on $^{\text{nat}}\text{Pb}$

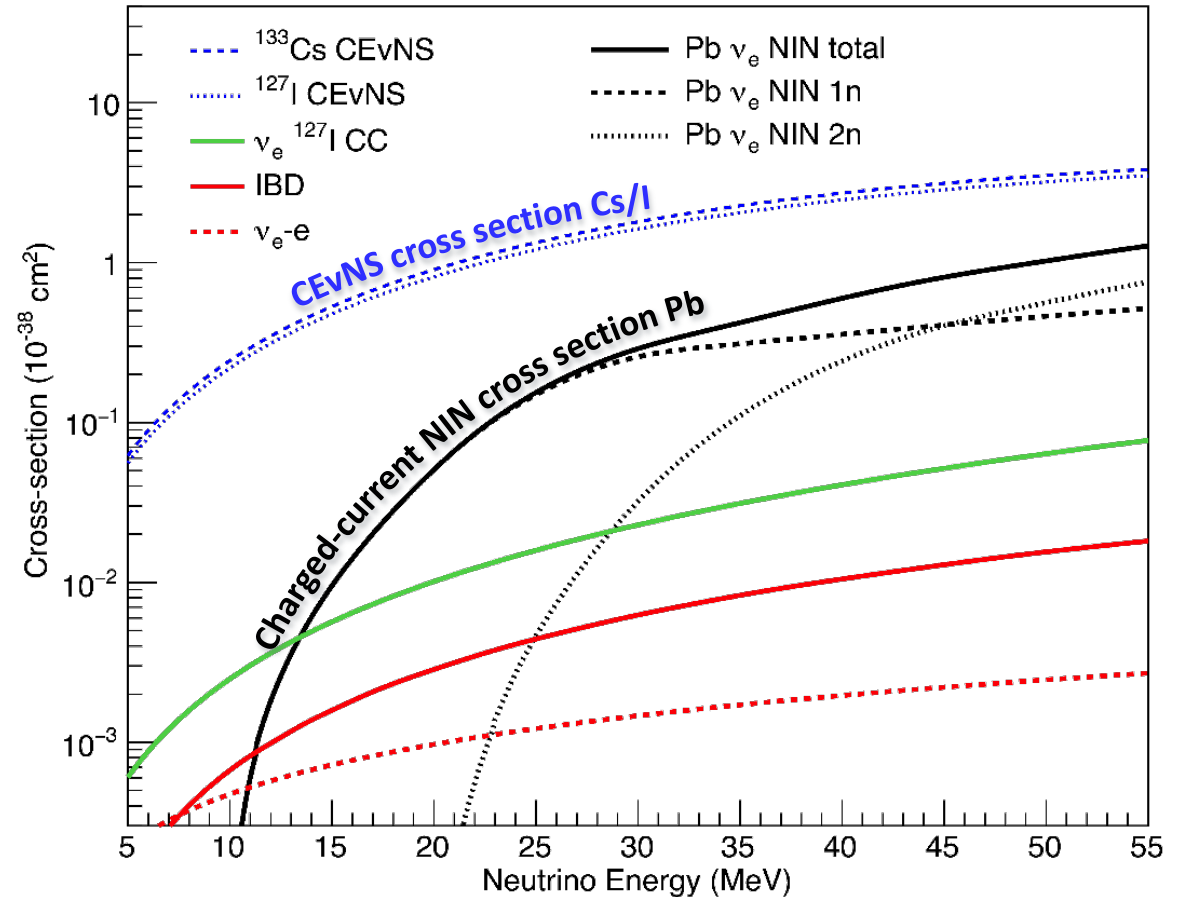
# Motivation for Measuring NINs

- Neutrino interactions in shielding of COHERENT's detectors could present beam-related background
  - Neutrino interactions can generate excited nuclei that de-excite by emitting neutrons
  - Produced neutrons follow the timing distribution of the neutrinos, and can produce low energy nuclear recoils in detectors



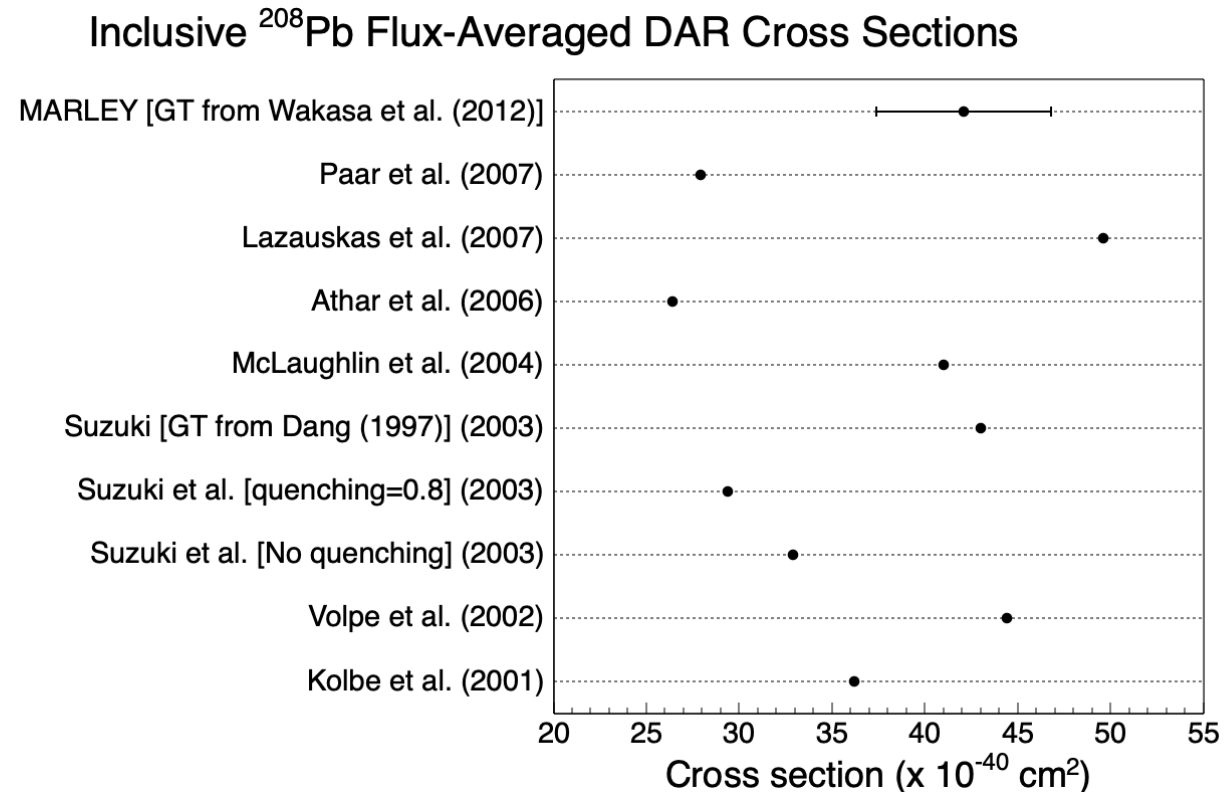
# Motivation for Measuring NINs

- Neutrino interactions in shielding of COHERENT's detectors could present beam-related background
  - Neutrino interactions can generate excited nuclei that de-excite by emitting neutrons
  - Produced neutrons follow the timing distribution of the neutrinos, and can produce low energy nuclear recoils in detectors
- Cross section expected to be lower than CEvNS, but previously unmeasured



# Motivation for Measuring NINs

- Neutrino interactions in shielding of COHERENT's detectors could present beam-related background
  - Neutrino interactions can generate excited nuclei that de-excite by emitting neutrons
  - Produced neutrons follow the timing distribution of the neutrinos, and can produce low energy nuclear recoils in detectors
- Cross section expected to be lower than CEvNS, but previously unmeasured
  - Variations in calculations



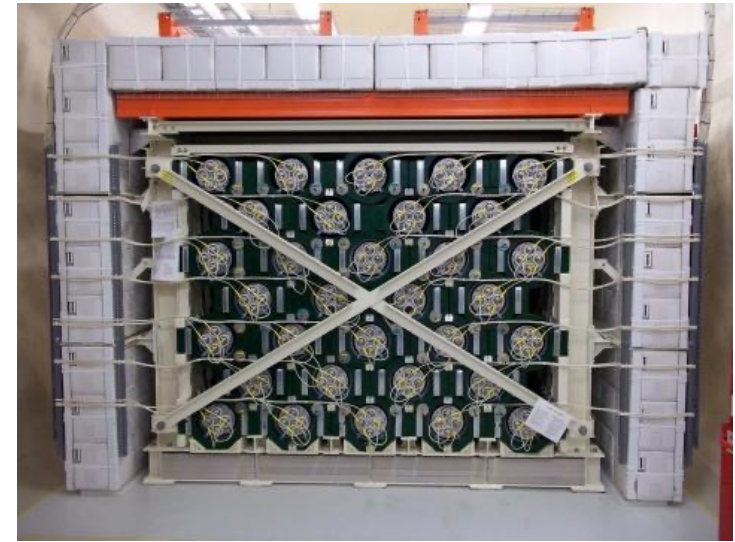
# Motivation for Measuring NINs

- Neutrino interactions in shielding of COHERENT's detectors could present beam-related background
  - Neutrino interactions can generate excited nuclei that de-excite by emitting neutrons
  - Produced neutrons follow the timing distribution of the neutrinos, and can produce low energy nuclear recoils in detectors
- Cross section expected to be lower than CEvNS, but previously unmeasured
  - Variations in calculations
  - Much greater mass of shielding than CEvNS detectors themselves

CEvNS Target	Shielding
14.6 kg CsI[Na]	2,200 kg lead
24 kg liquid argon	11,000 kg lead
16 kg Ge	3,400 kg lead
2,425 kg NaI	17,000 kg iron and lead

# Motivation for Measuring NINs

- Neutrino interactions in shielding of COHERENT's detectors could present beam-related background
  - Neutrino interactions can generate excited nuclei that de-excite by emitting neutrons
  - Produced neutrons follow the timing distribution of the neutrinos, and can produce low energy nuclear recoils in detectors
- Cross section expected to be lower than CEvNS, but previously unmeasured
  - Variations in calculations
  - Much greater mass of shielding than CEvNS detectors themselves
- Primary mechanism for HALO to detect supernova neutrinos



[<https://www.triumf.ca/research-highlights/experimental-result/halo-operational-snolab>]

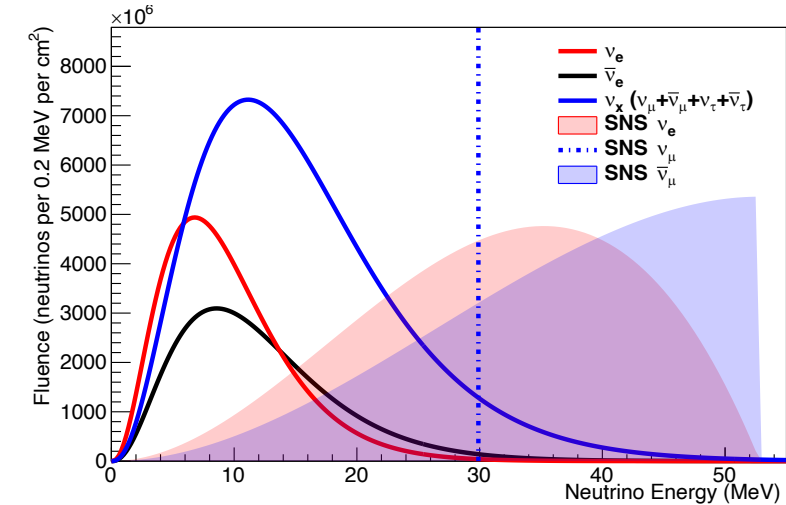
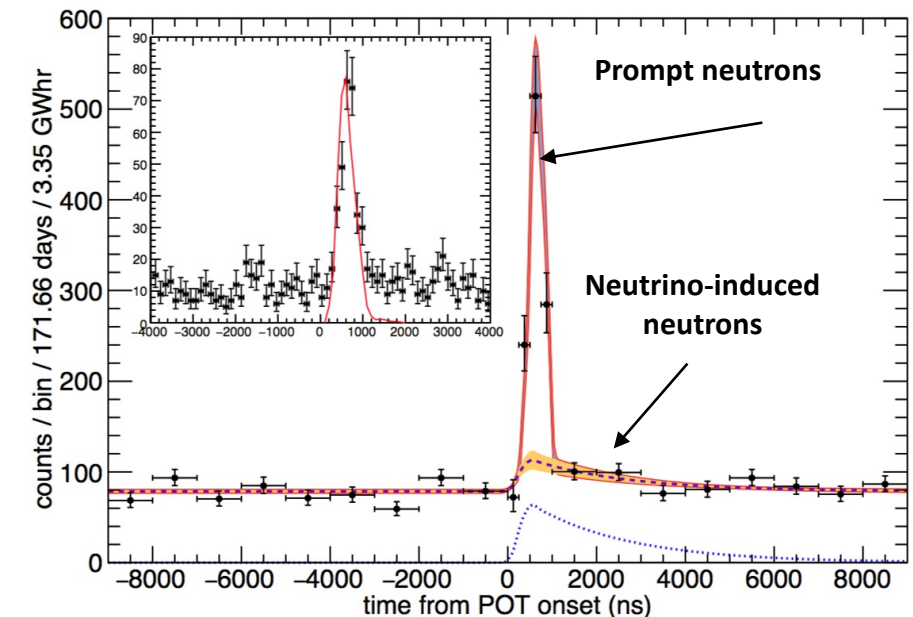


[image courtesy of K. Scholberg]

# Initial Attempt—Eljen Cell Detector

- In 2015, prior to deployment of CsI[Na] CEvNS detector, two 1.5-L liquid scintillators deployed inside its shielding
  - 2,200kg of Pb shielding  $\sim$ 20m from target
  - Exposure of 171.7 days (3.35 GWhr)
  - Threshold of 30 keVee
- Best fit of non-zero NIN component at  $2.9\sigma$ 
  - $0.97 \pm 0.33$  neutrons produced/GWhr/kg of Pb
  - $\sim 1.7x$  lower than predicted in McLaughlin, G.C. Phys. Rev. C **70** 4 (2004)
- Not a major background for CEvNS in CsI
  - With additional HDPE shielding added inside lead,  $\sim 47x$  lower than CEvNS signal!

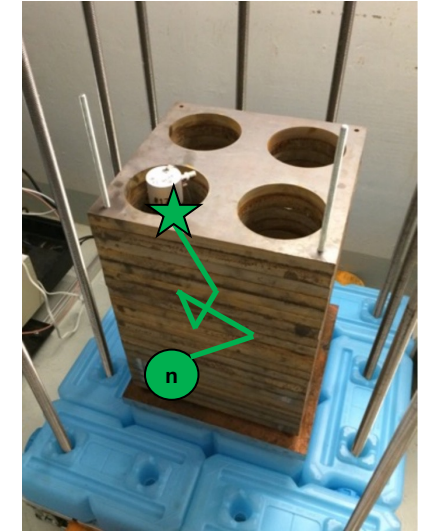


[D. Akimov, et al., Science 357 (2017)]



# The Lead Neutrino Cube

- Two dedicated NIN detectors at SNS
  - 900-kg Pb—deployed in 2015
  - 700-kg Fe—deployed in 2017
- NINs produced in lead/iron have small but non-zero efficiency to make their way to LS cells, identified as neutrons using PSD
- Muon veto panels surround targets to reject muon-induced neutrons
- Water shielding reduces steady-state, beam-related neutrons
- Focus on delayed neutrino window, CC cross section expected to be larger than NC, free of prompt beam-related neutron (BRN) background



LS detectors  
Pb target

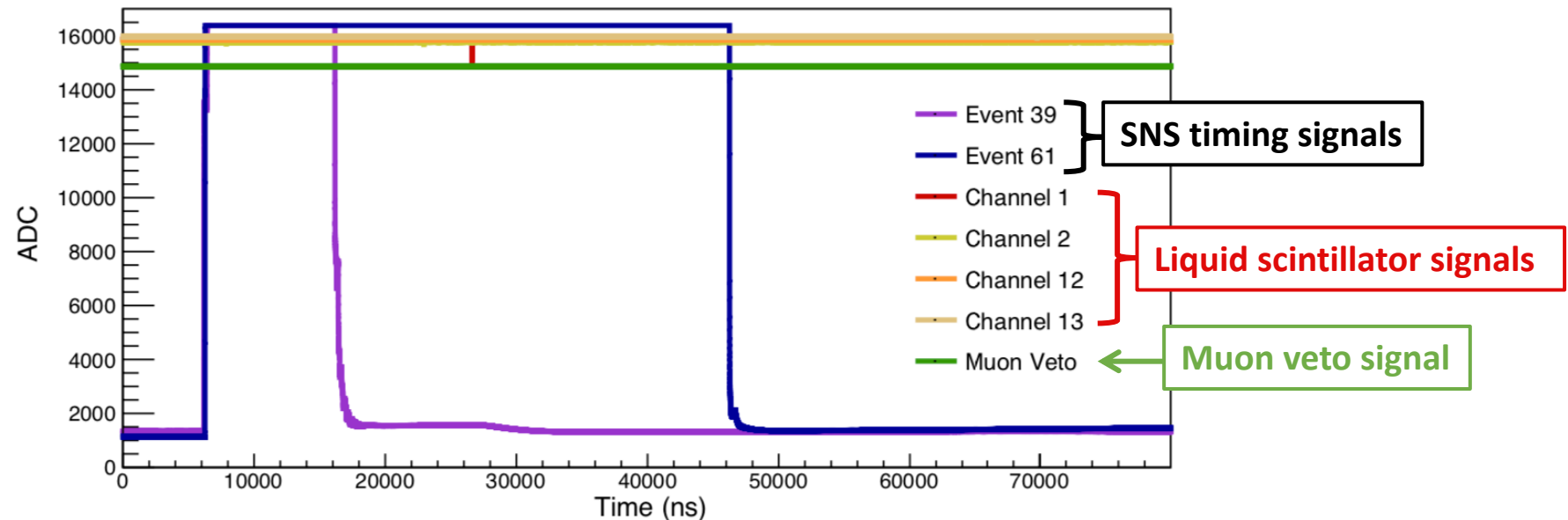


Muon veto panels  
Water shielding



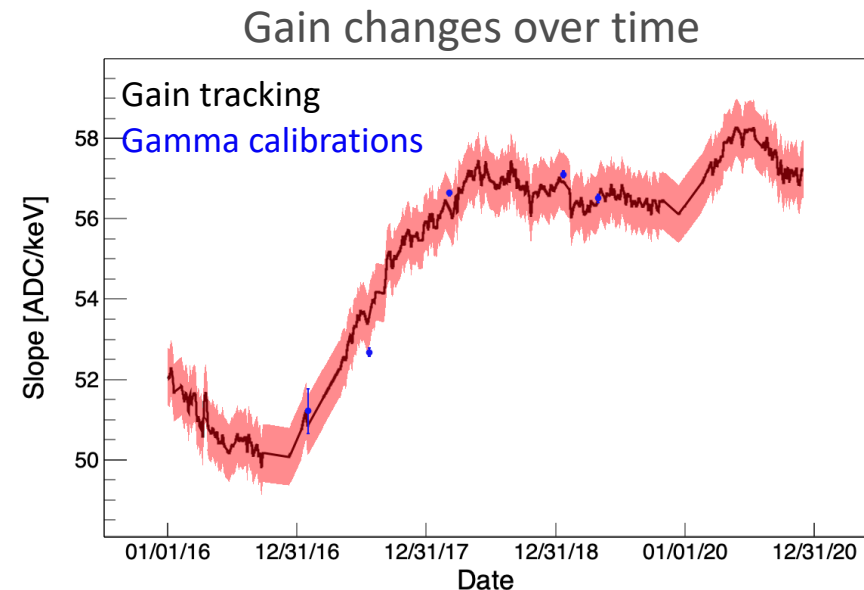
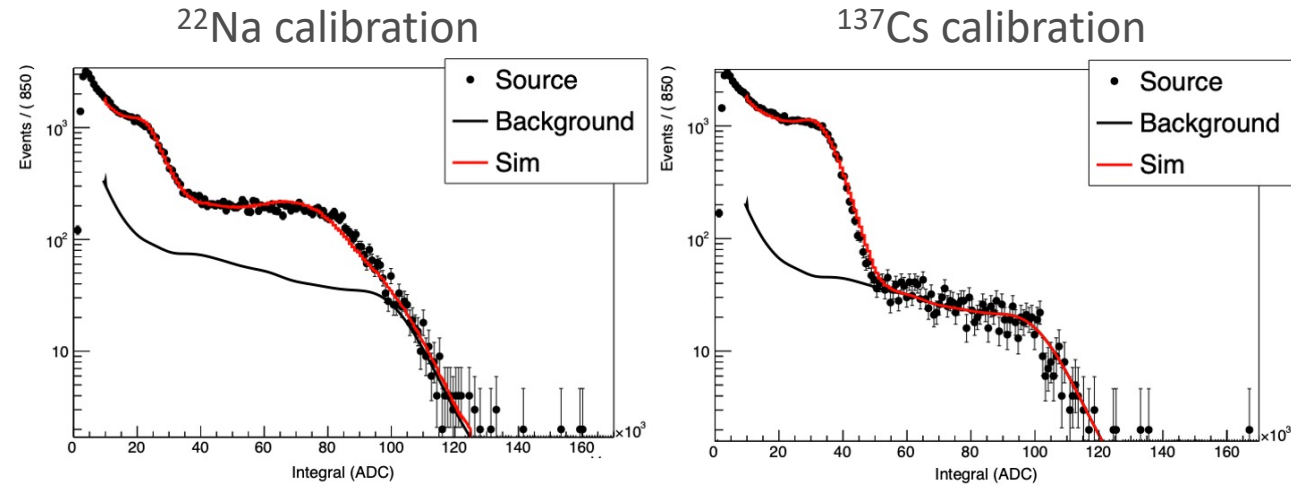
# Data Acquisition Scheme

- DAQ record coincidences between SNS timing signals and internal triggers within  $20\mu\text{s}$  window, record all channels
- Waveform reconstruction code:
  - Filter waveforms to remove long-timescale oscillations in baseline
  - Identify pulses, integrate for energy and PSD parameter
  - Hold-off time to remove electronic ringing artifacts
  - In software, correlate LS pulses with vetoes, SNS timing pulses
- Events within a  $14\mu\text{s}$  window around the SNS timing signal blinded



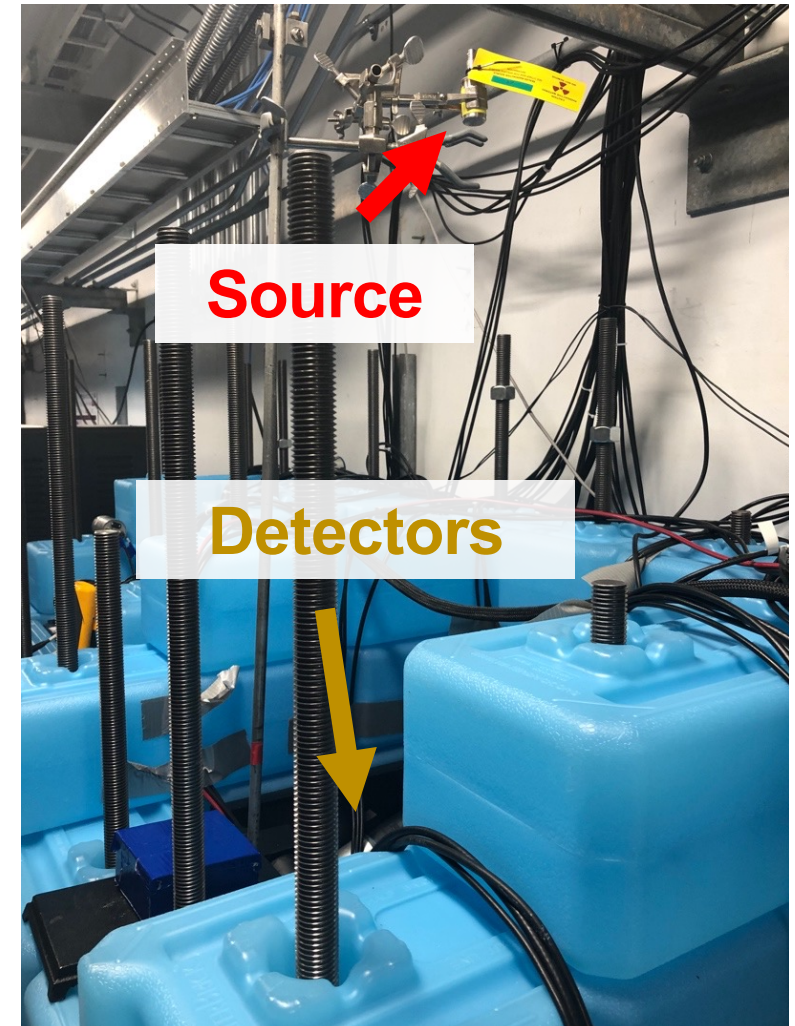
# Gamma Calibrations

- Calibrations performed with gammas source ( $^{22}\text{Na}$ ,  $^{137}\text{Cs}$ ,  $^{133}\text{Ba}$ ,  $^{60}\text{Co}$ ) several times throughout detector operations
- Source and detector simulated in MCNP, fit to data allowing energy-resolution and ADC-to-keV calibration parameters to float
- Between calibrations, background spectrum fit (largely due to  $^{40}\text{K}$ ) to track gain on shorter time scales



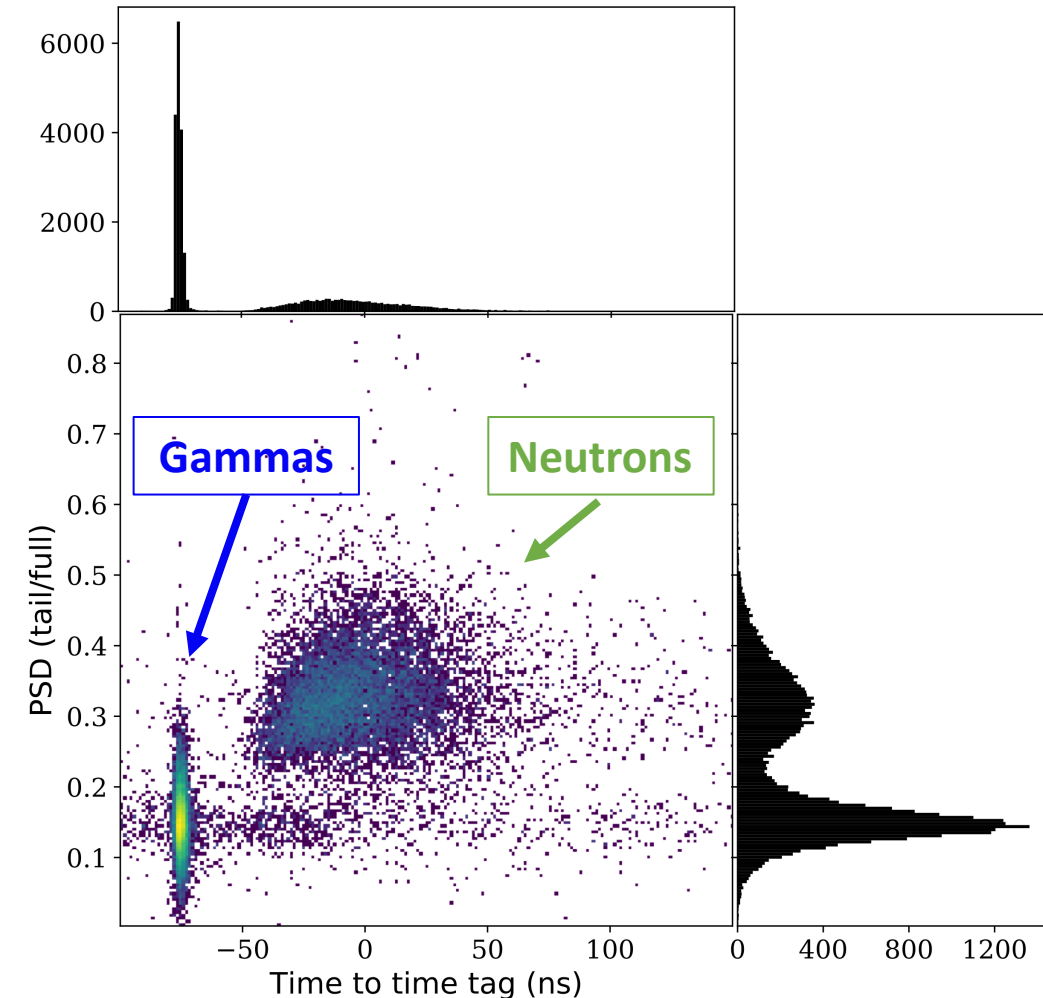
# Neutron Calibrations

- *in-situ* run performed with time-tagged  $^{252}\text{Cf}$  neutron source
- Time-tagged signal replaced SNS timing signal in DAQ, shielding removed to expose detectors to source, otherwise identical to running configuration



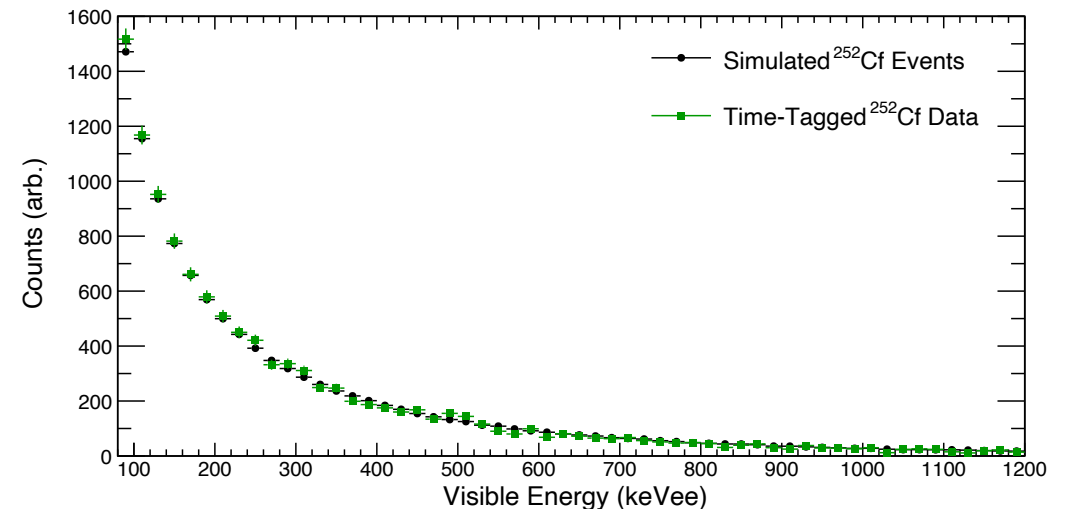
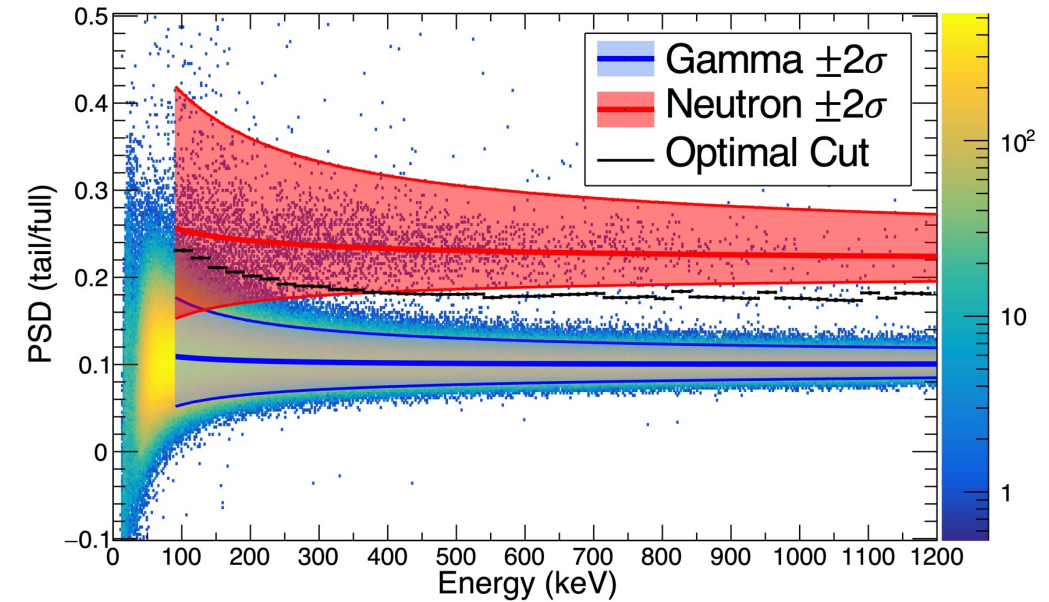
# Neutron Calibrations

- *in-situ* run performed with time-tagged  $^{252}\text{Cf}$  neutron source
- Time-tagged signal replaced SNS timing signal in DAQ, shielding removed to expose detectors to source, otherwise identical to running configuration
- Produced clean population of gammas, neutrons for understanding thresholds, optimizing PSD parameter



# Neutron Calibrations

- *in-situ* run performed with time-tagged  $^{252}\text{Cf}$  neutron source
- Time-tagged signal replaced SNS timing signal in DAQ, shielding removed to expose detectors to source, otherwise identical to running configuration
- Produced clean population of gammas, neutrons for understanding thresholds, optimizing PSD parameter
- Develop neutron PSD cut
- Compare data to simulation to ensure we understand energy response



# MARLEY

- Used MARLEY\* to generate signal predictions for inelastic neutrino-nucleus interactions at the SNS
- **Model of Argon Reaction Low Energy Yields**—originally designed for  $^{40}\text{Ar}$ , but can be used with other nuclei
- Handles allowed components of inelastic neutrino-nucleus reactions at low energies
  - Forbidden transitions play larger role at higher energies

$$\frac{d\sigma}{d\cos\theta_\ell} = \frac{G_F^2 |U_{ud}|^2}{2\pi} F_C \left[ \frac{E_i E_f}{s} \right] E_\ell |\vec{p}_\ell| \left[ (1 + \beta_\ell \cos\theta_\ell) B(F_-) + \left(1 - \frac{1}{3} \beta_\ell \cos\theta_\ell\right) B(GT_-) \right]$$

- Inputs are Gamow-Teller strength distributions
  - Calculate theoretically or measure via charge-exchange reactions—(p,n) or ( $^3\text{He}$ ,t)

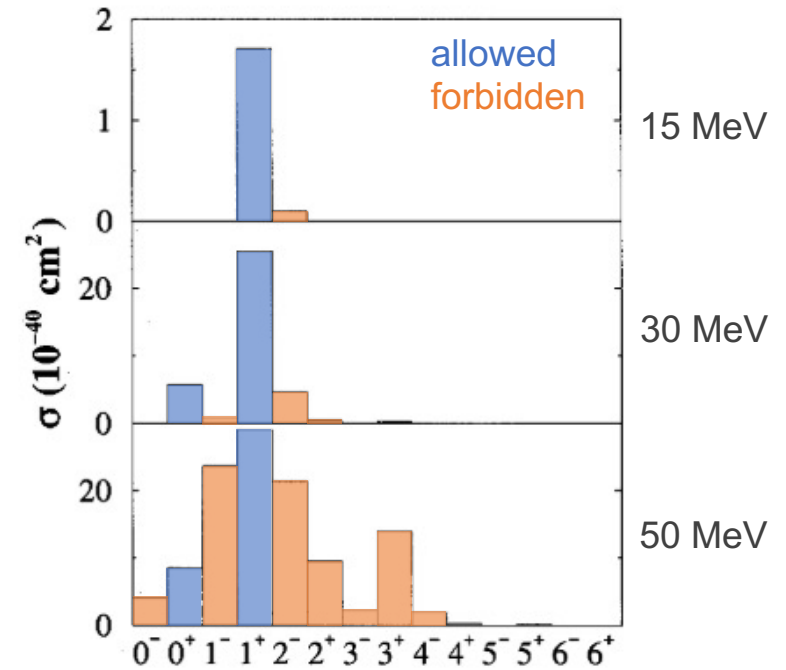


FIG. 3. Contribution of the different multiplicities to the differential  $^{208}\text{Pb}(\nu_e, e^-)^{208}\text{Bi}$  cross section ( $10^{-40} \text{ cm}^2$ ) of Fig. 1 for  $E_{\nu_e} = 15 \text{ MeV}$  (up),  $30 \text{ MeV}$  (middle),  $50 \text{ MeV}$  (bottom).

[C. Volpe, et al., Phys. Rev. C **65** (2002)]

\*S. Gardiner, Simulating low-energy neutrino interactions with MARLEY, Comput. Phys. Commun. 269, 108123

# MARLEY for $^{208}\text{Pb}$

- Gamow-Teller strengths obtained from (p,n) measurement
  - Input  $B(\text{GT}^-)$  and  $B(\text{F})$  values into MARLEY along with electron neutrino DAR spectrum

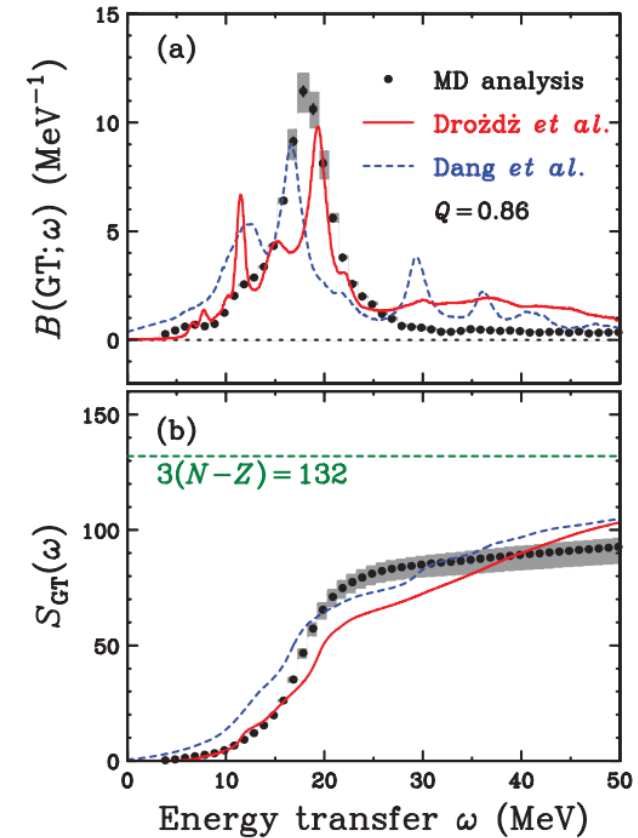


FIG. 16. (Color online) (a) The GT strength  $B(\text{GT}; \omega)$  and (b) its integrated  $S_{\text{GT}}(\omega)$  distributions obtained by MD analysis of the  $^{208}\text{Pb}(p, n)$  reaction. The bands represent the uncertainties arising from the selection of  $\alpha$  in Eq. (18). The solid and dashed curves are the theoretical predictions reported by Drożdż *et al.* [18] and Dang *et al.* [62], respectively, with a quenching factor  $Q = 0.86$  [13].

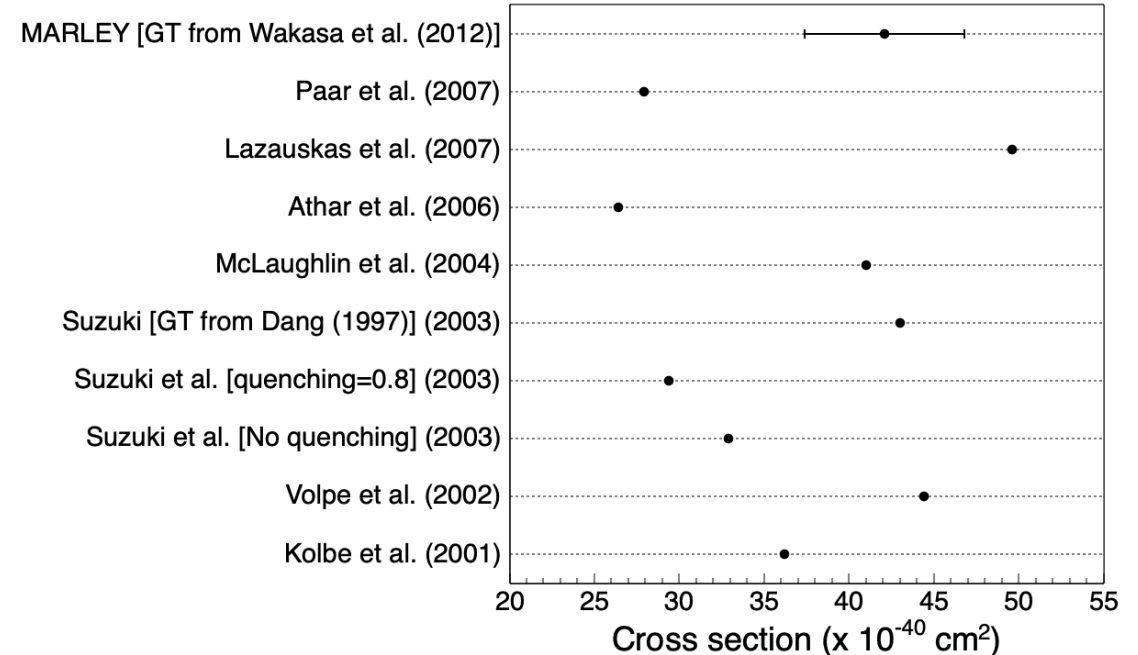
[T. Wakasa, et al., Phys Rev. C **85** (2012)]



# MARLEY for $^{208}\text{Pb}$

- Gamow-Teller strengths obtained from (p,n) measurement
  - Input  $B(\text{GT}^-)$  and  $B(\text{F})$  values into MARLEY along with electron neutrino DAR spectrum
- MARLEY outputs cross sections, energies and multiplicities of emitted particles
  - Cross section for lead agrees well with existing theoretical calculations
  - Provides calculations for specific channels

Inclusive  $^{208}\text{Pb}$  Flux-Averaged DAR Cross Sections

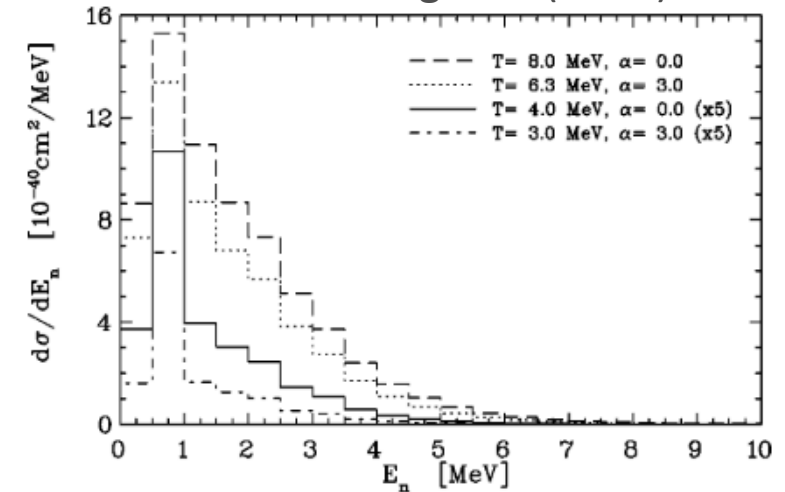


Channel	Cross section ( $\times 10^{-40} \text{ cm}^2$ )
$^{208}\text{Pb}(\nu_e, X)$	42.1
$^{208}\text{Pb}(\nu_e, e^- + n)^{207}\text{Bi}$	31.6
$^{208}\text{Pb}(\nu_e, e^- + 2n)^{206}\text{Bi}$	7.7
$^{208}\text{Pb}(\nu_e, e^- + 3n)^{205}\text{Bi}$	0.4

# MARLEY for $^{208}\text{Pb}$

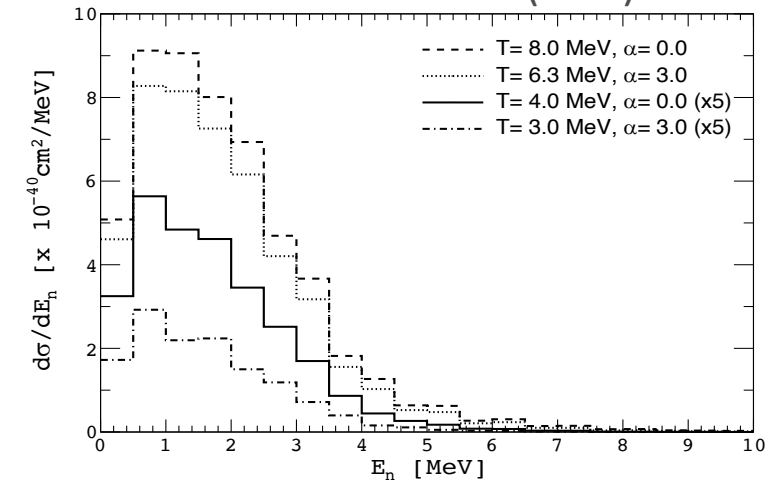
- Gamow-Teller strengths obtained from (p,n) measurement
  - Input  $B(\text{GT}^-)$  and  $B(\text{F})$  values into MARLEY along with electron neutrino DAR spectrum
- MARLEY outputs cross sections, energies and multiplicities of emitted particles
  - Cross section for lead agrees well with existing theoretical calculations
  - Provides calculations for specific channels
- Similar neutron energy spectrum as E. Kolbe & K. Langanke, Phys. Rev. C **64** (2001) for supernova neutrinos
  - No published neutron spectrum from DAR neutrinos w/o MARLEY

Kolbe & Langanke (2001)



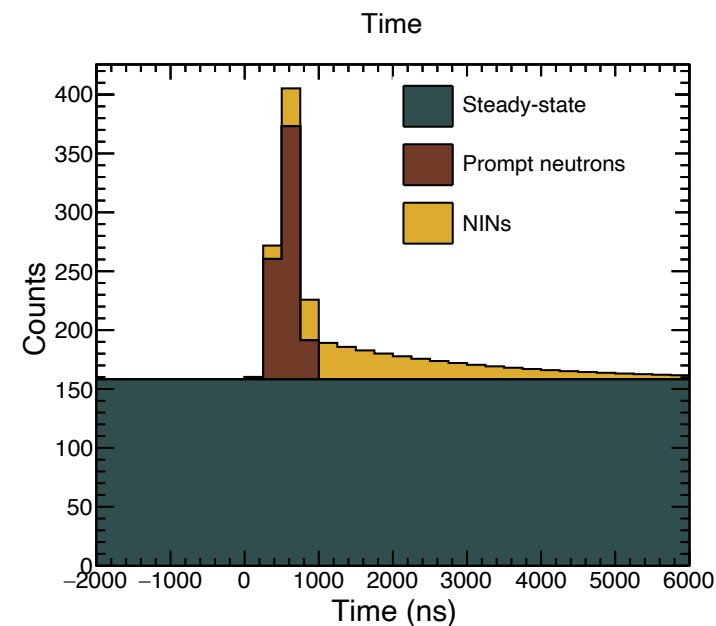
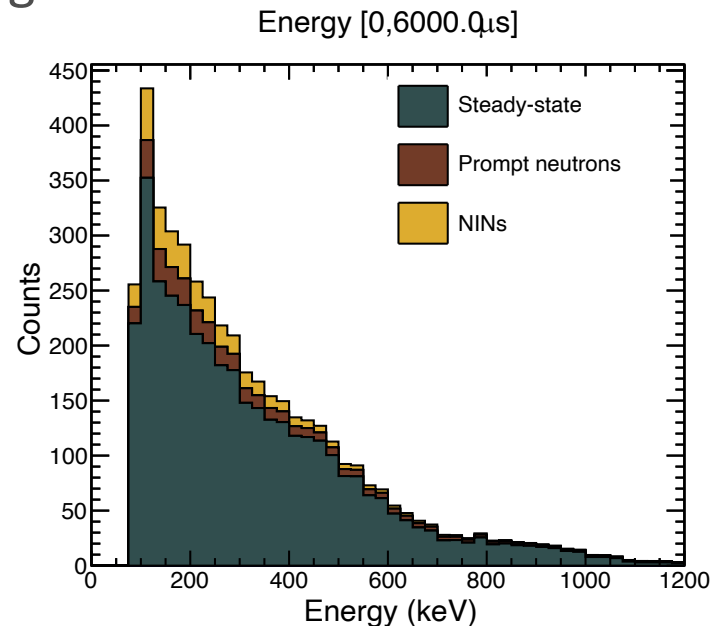
[E. Kolbe & K. Langanke, Phys. Rev. C **64** (2001)]

MARLEY + Wakasa  $B(\text{GT}^-)$  data



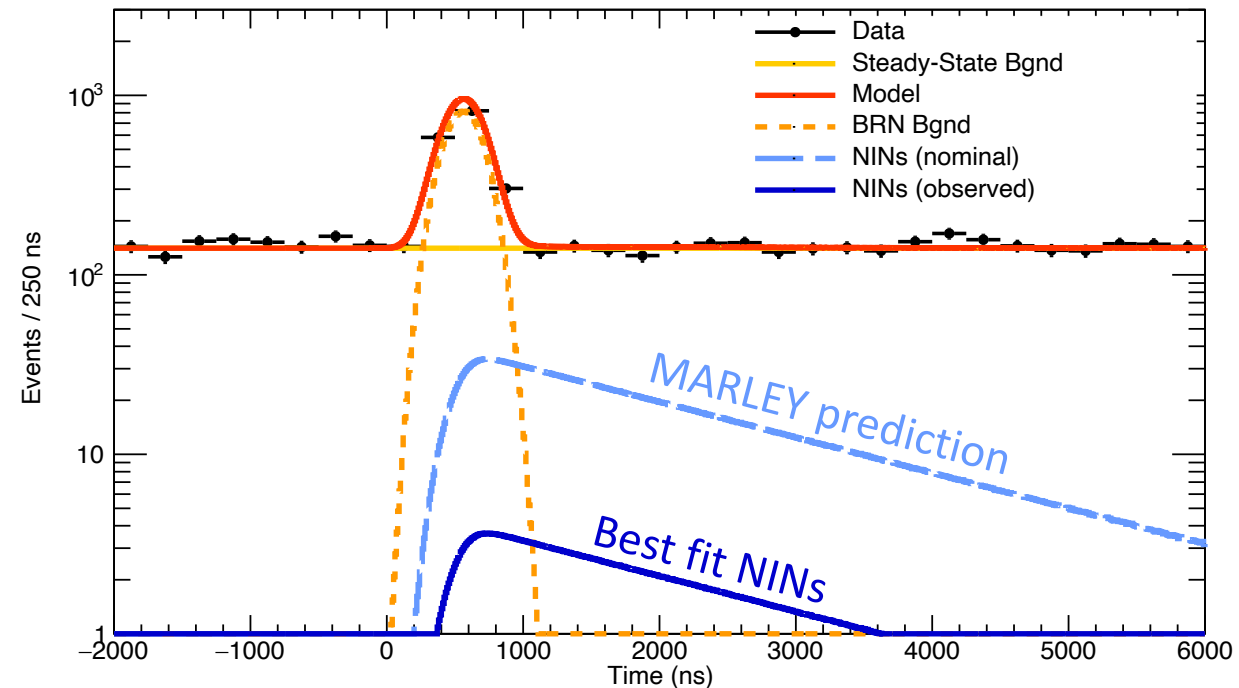
# PDFs

- MARLEY events simulated in MCNP, GEANT4 to determine efficiency for NINs arriving in detector of 18.8%
- Apply measured trigger threshold, energy resolution, PSD cut, to arrive at an efficiency of detecting NINs of 3.3%
- One-dimensional (time-only) fit to data
- Using MARLEY's predictions, expect 346 charged-current NIN events with cuts
  - Approx.  $5\sigma$  significance with nominal cross section



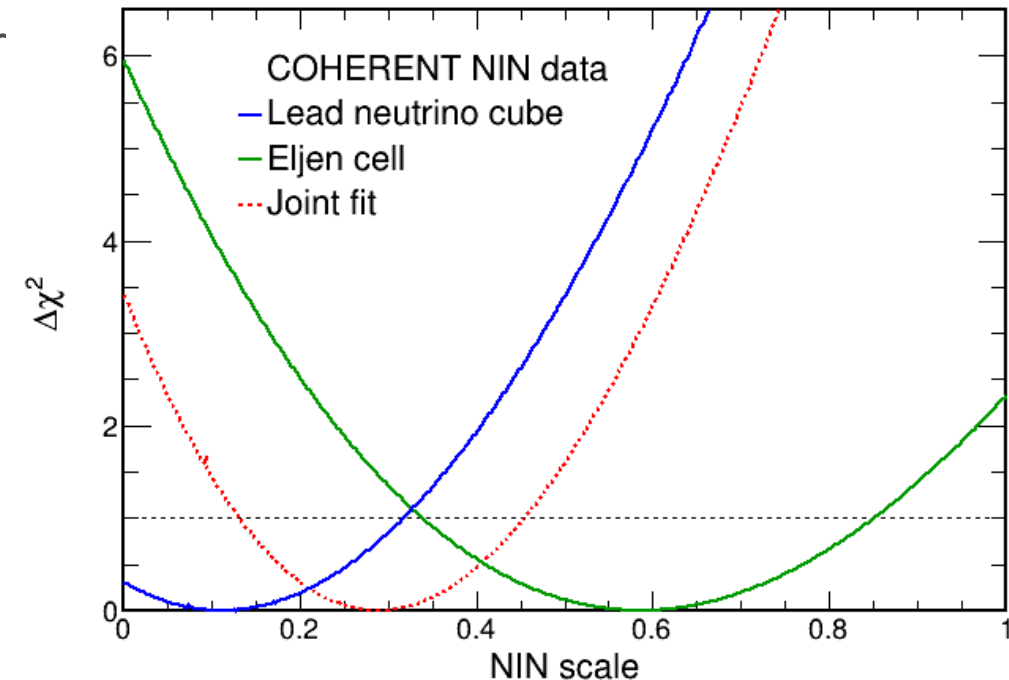
# Unblinded Results

- Best fit of  $36_{-36}^{+72}$  events compared to expected 346 events
  - Cross section lower than expected
- Post-unblinding checks:
  - Purity of lead target—stamped as >99.99% pure, density consistent with lead
  - Detector sensitivity to neutrons over lifetime—BRNs compared to delivered beam power show excellent agreement
  - PSD cut extended to lower energies where uncertainties more difficult to quantify due to presence of Cherenkov events—increased number of events, but suppression of cross section still observed



# Combined Fit with Eljen Cell Data

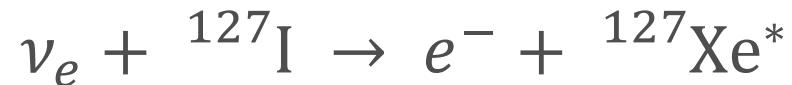
- Data from Eljen-cell detector reanalyzed
  - Used MARLEY framework for generating predictions
  - Allowed additional smearing term for BRN timing due to dispersion effects (included in lead neutrino cube fit)
  - Improved predictions for neutrino flux based on beam power and energy (D. Akimov, et al., arXiv:2109.11049 (2021))
- Combined fit yields MARLEY cross section suppressed by a factor of  $0.29^{+0.17}_{-0.17}$ 
  - $1.8\sigma$  significance,  $>4\sigma$  disagreement with MARLEY model
- Open questions:
  - Is neutron emission channel suppressed?
    - Study inclusive lead charged-current cross section
    - Can do within COHERENT, also external plans (arXiv:2205.11769)
  - Are emitted neutrons lower in energy than predicted?
    - Study lead NIN cross section with capture-gated detector
  - Is the NIN cross section suppressed for other targets?
    - Study NIN cross section with different target (Fe neutrino cube)



# Inclusive Neutrino-Nucleus Scattering on $^{127}\text{I}$

# Motivation for Measuring $^{127}\text{I}$ CC Interactions

- Initial motivation from W. C. Haxton, Phys. Rev. Lett **60** (1988), proposing radiochemical experiment using  $^{127}\text{I}$  for solar neutrino detection



- Low threshold gives access to  ${}^7\text{Be}$  solar neutrinos, larger cross section than for  ${}^{37}\text{Cl}$
- Resulting  ${}^{127}\text{Xe}$  has long half-life, use similar radiochemical technique as used for  ${}^{37}\text{Cl}$
- Engel, et al. pointed out the cross section depends on  $g_A$ 
  - Suppression of  $g_A$  important for interpreting  $0\nu\beta\beta$  matrix elements, half-lives
  - Can potentially test quenching at momentum transfer not available through beta-decay experiments

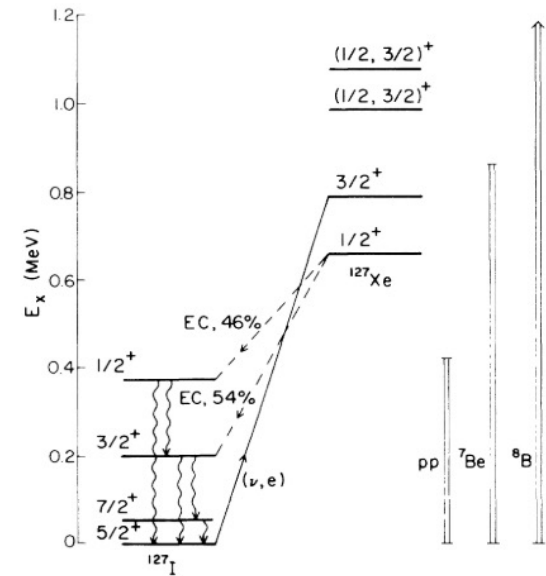


FIG. 1. Level scheme showing weak transitions between  $^{127}\text{I}$  and  $^{127}\text{Xe}$ .

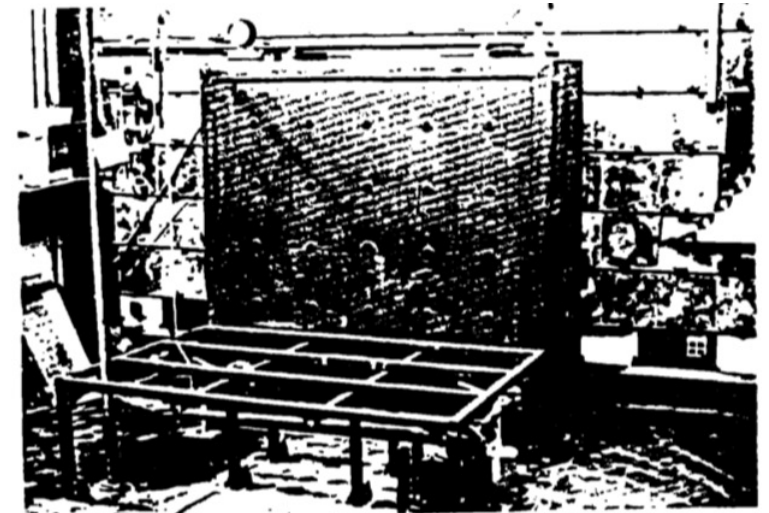
[W. C. Haxton, Phys. Rev. Lett **60** (1988)]

$J^\pi$	$g_A = -1.0$	$g_A = -1.26$
0 <sup>+</sup>	0.096	0.096
0 <sup>-</sup>	0.00001	0.00002
1 <sup>+</sup>	1.017	1.528
1 <sup>-</sup>	0.006	0.008
2 <sup>+</sup>	0.155	0.213
2 <sup>-</sup>	0.693	1.055
3 <sup>+</sup>	0.149	0.171
3 <sup>-</sup>	0.017	0.025
total	2.098	3.096

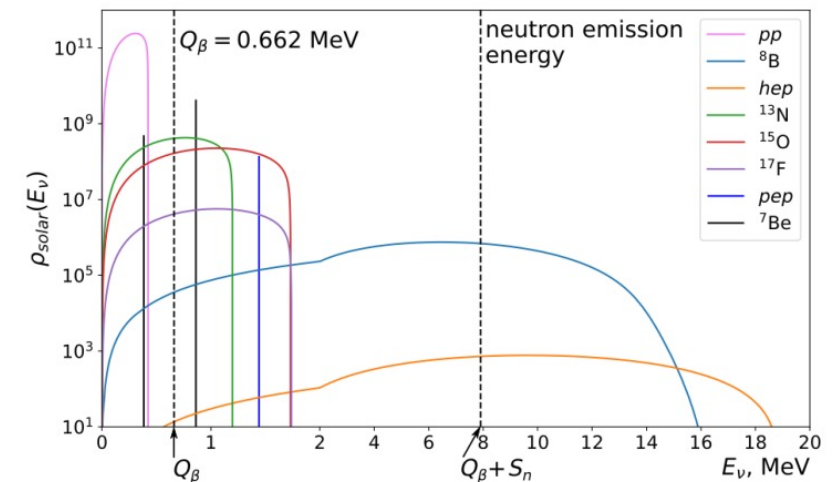
[J. Engel, S. Pittel, & P. Vogel, Phys. Rev. C **50** (1994)]

# Motivation for Measuring $^{127}\text{I}$ CC Interactions

- Exclusive cross section to  $^{127}\text{Xe}_{\text{bound}}$  measured at LAMPF in the 1990s with radiochemical approach
- Reported flux-averaged cross section of  $\sigma = 2.84 \pm 0.91(\text{stat}) \pm 0.25(\text{sys}) \times 10^{-40} \text{ cm}^2$ 
  - Only measured cross section to bound states of  $^{127}\text{Xe}$ —majority of neutrinos at DAR sources have energy above neutron emission threshold
- Suggested repetition with electronic NaI detector to measure energy-dependence of cross section
- Recently interest in looking at  $^{126}\text{Xe}/^{127}\text{Xe}$  ratio for comparing  $^7\text{Be}$  to  $^8\text{B}/\text{HEP}$  neutrinos



[B. T. Cleveland, et al., 23rd Int. Cosmic Ray Conf. 3 (1993)]

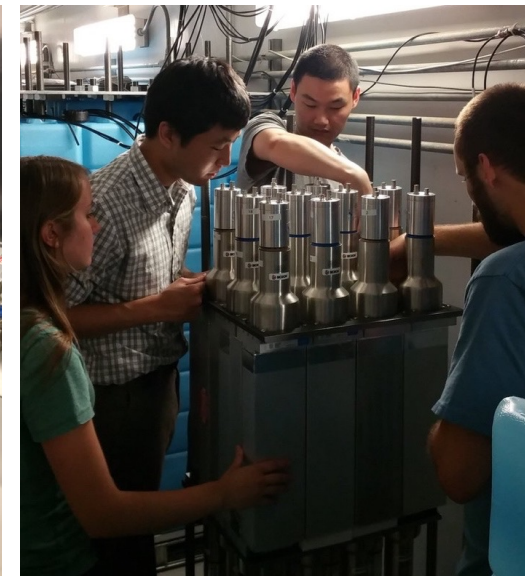
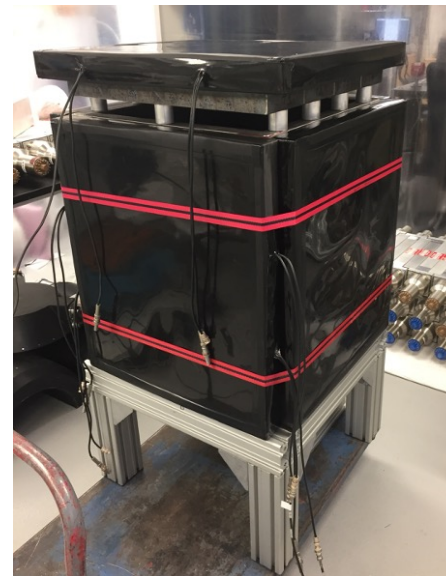
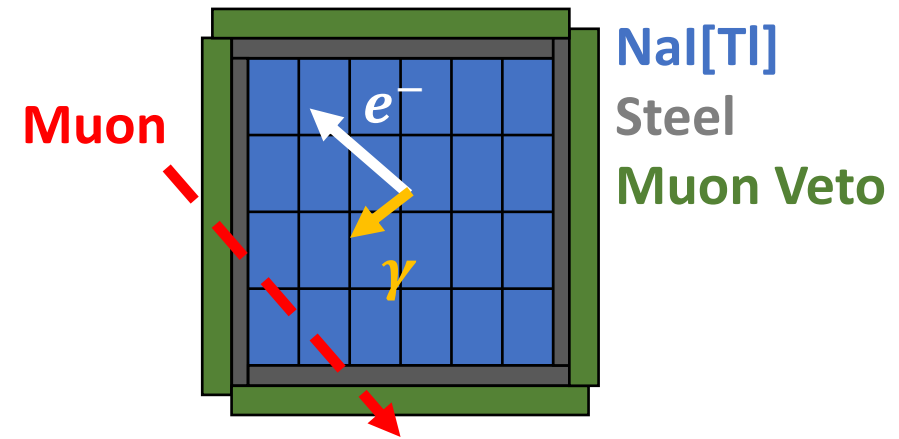


[Y. S. Lutostansky, et al., arXiv:2103.12325 (2021)]



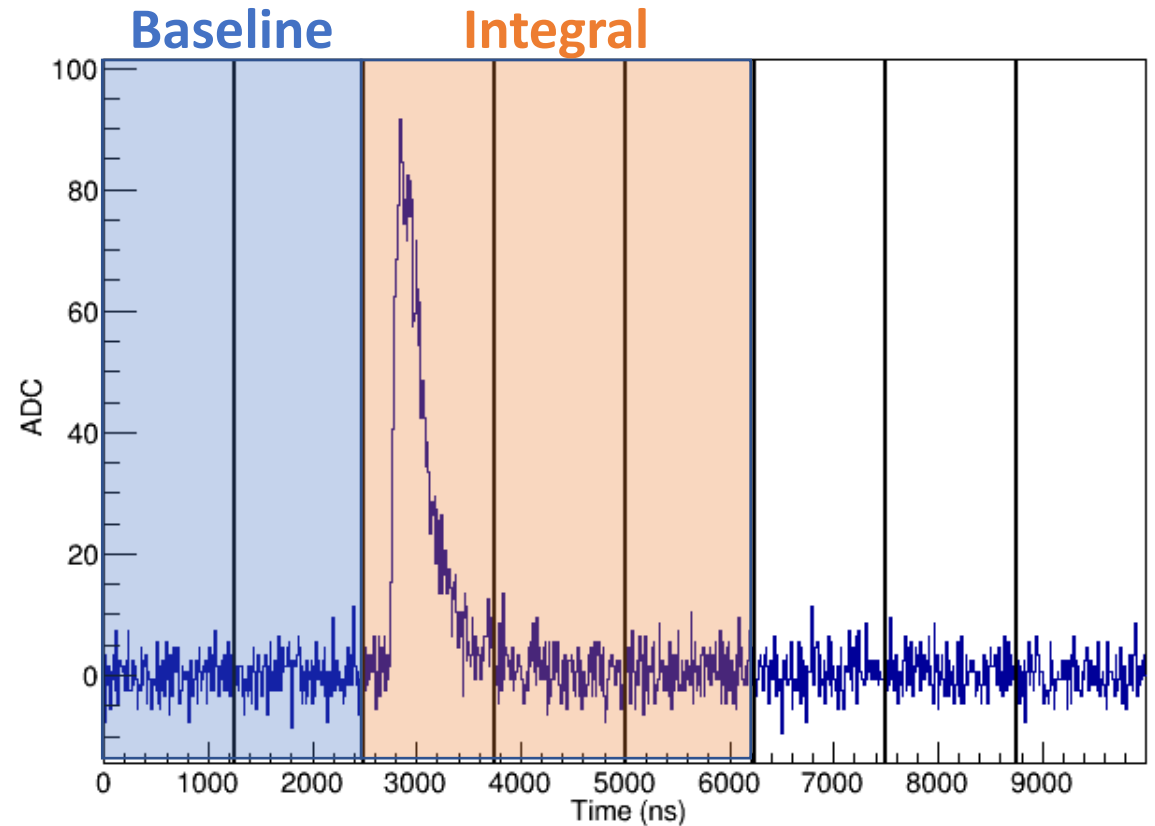
# NaIvE-185 Detector

- NaI neutrino Experiment (**NaIvE**) designed to measure the inclusive charged-current cross section, energy-dependence
- Twenty-four 7.7-kg NaI[Tl] scintillator detectors (185-kg mass), deployed 2016
- Signal is “large-energy” (10-55 MeV) depositions in delayed neutrino window
- Muon veto panels to reduce cosmic muons
- 1.5” steel between NaI and veto panels to avoid vetoing signal
- Detector also used as prototype for ton-scale NaI CEvNS detector



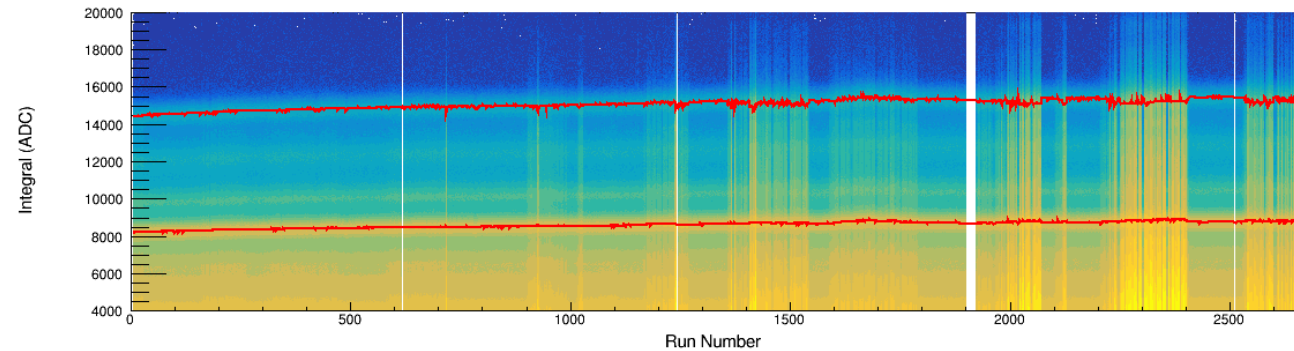
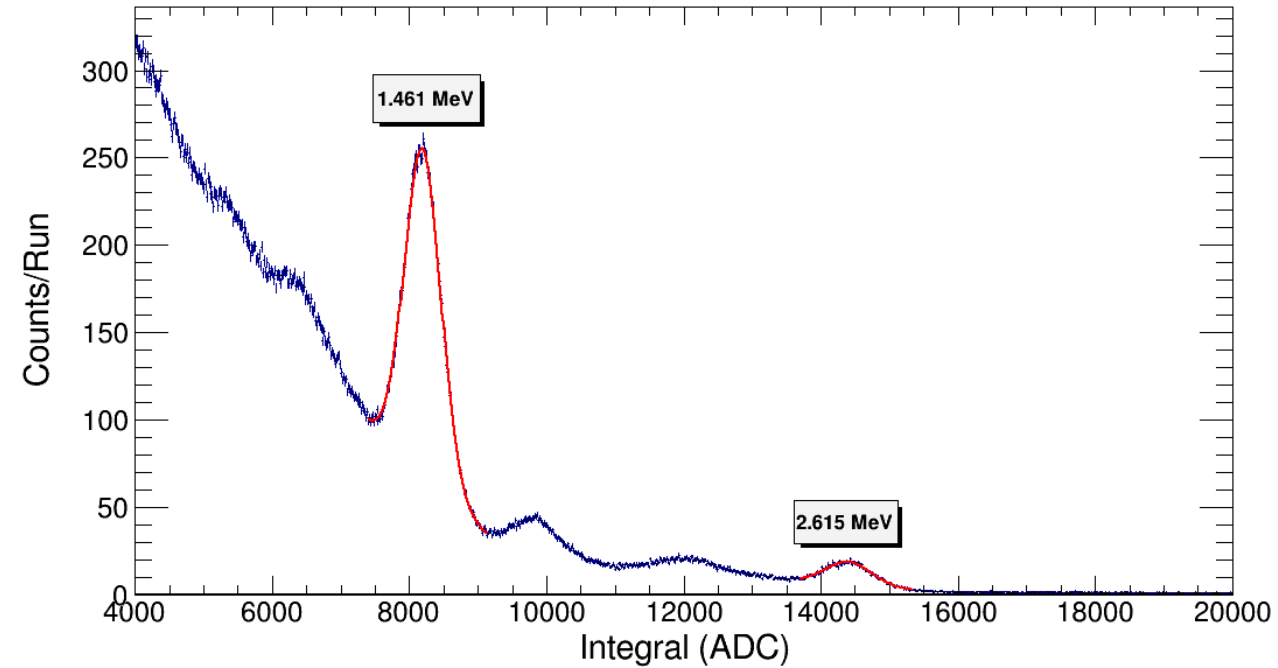
# Data Acquisition System

- Detector uses digitizer trigger to record scintillation in any NaI channel above a threshold (500-900 keV)
- Integrated PMT charge recorded in eight timing windows (accumulators) around the pulse to determine baseline, integral
- Muon veto panels, SNS timing pulses trigger independently, timing correlation done in software
  - Data within  $-2\mu\text{s}$  to  $+20\mu\text{s}$  of SNS timing signal blinded



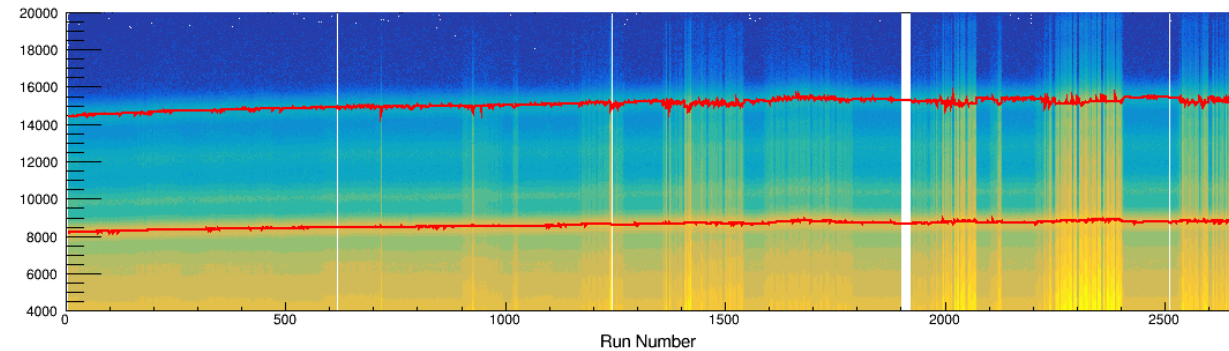
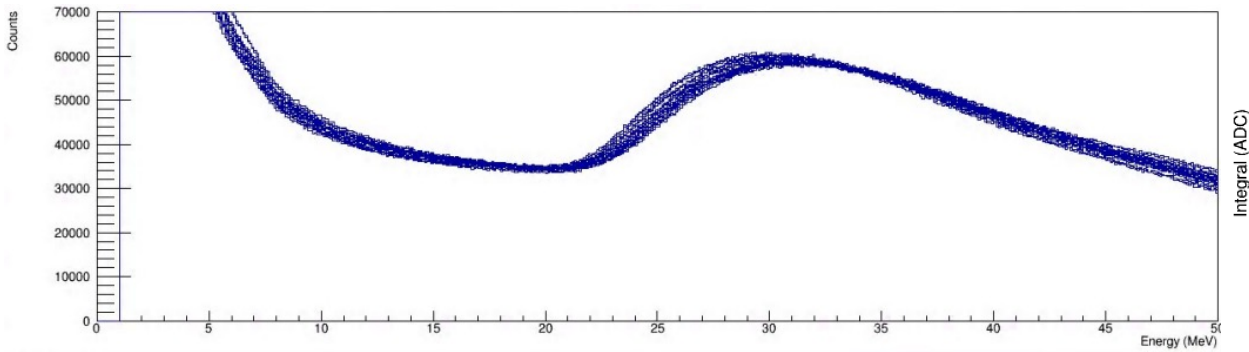
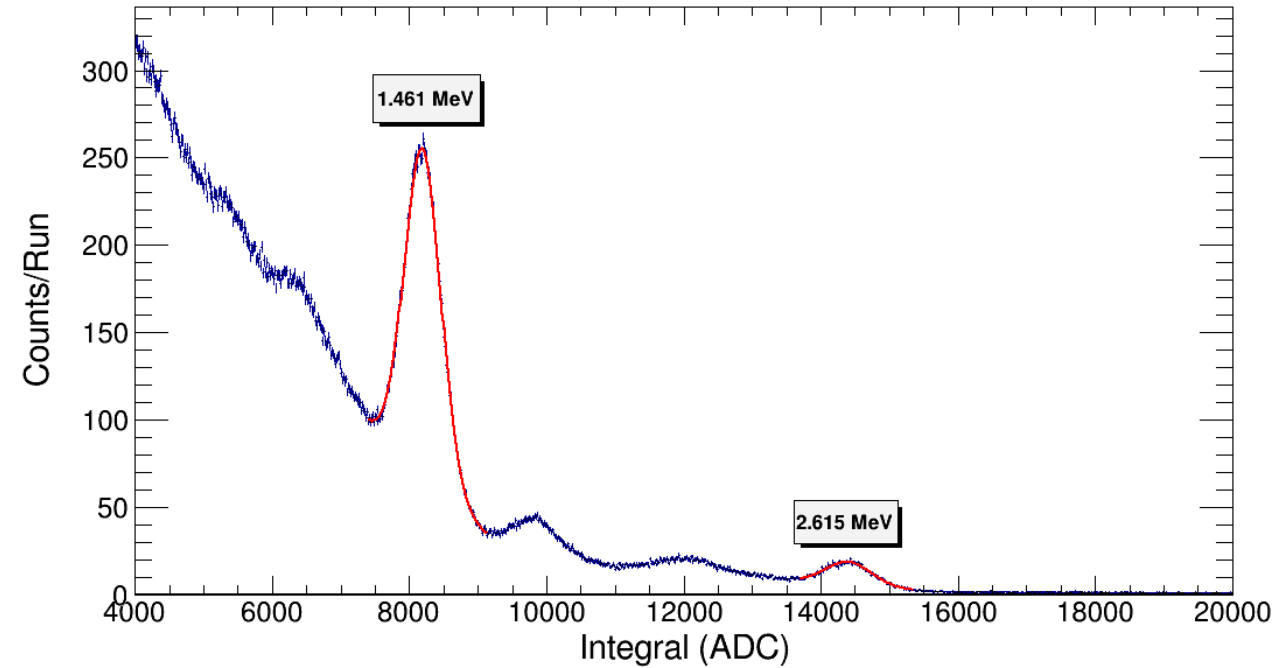
# Intrinsic Background Calibrations

- Calibrate each NaI channel based on  $^{40}\text{K}$  and  $^{208}\text{Tl}$  intrinsic backgrounds
  - Track gain changes over time, measure energy resolution in crystals



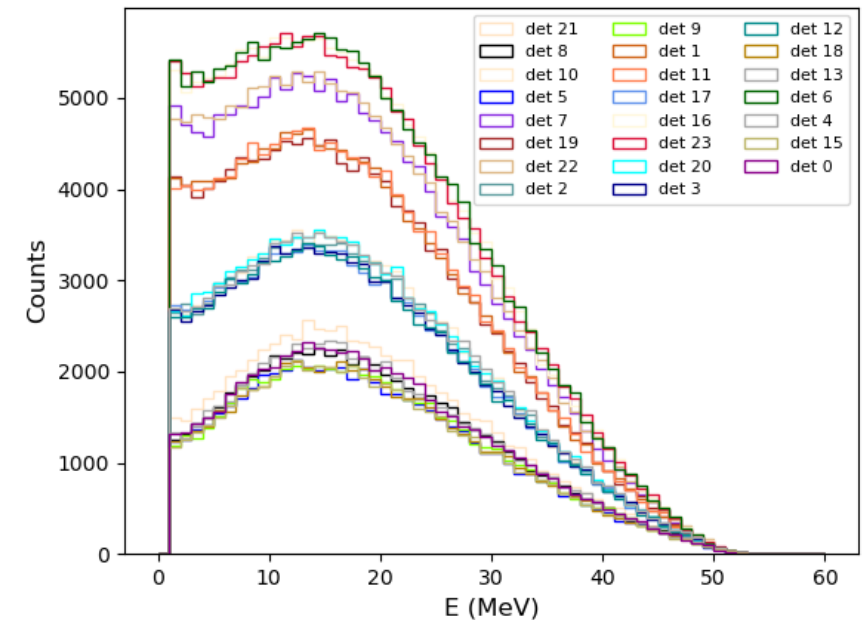
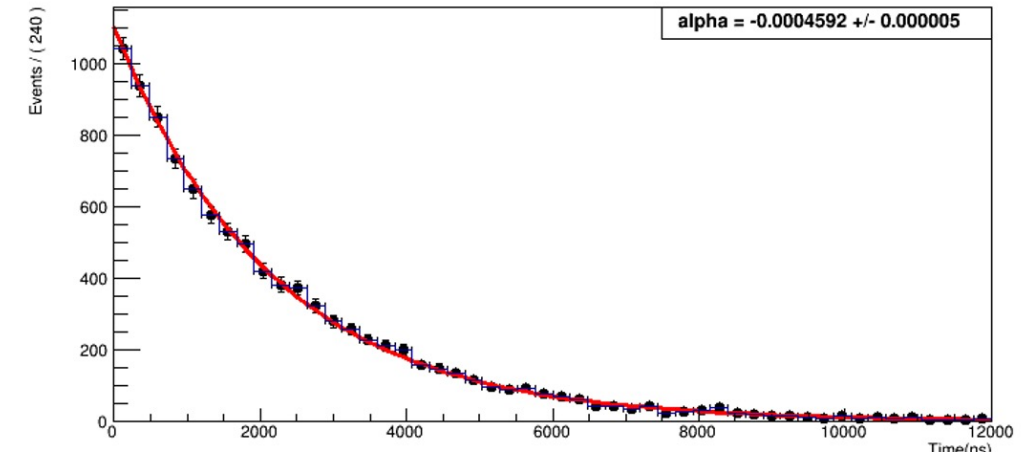
# Intrinsic Background Calibrations

- Calibrate each NaI channel based on  $^{40}\text{K}$  and  $^{208}\text{Tl}$  intrinsic backgrounds
  - Track gain changes over time, measure energy resolution in crystals
- Extending calibration to higher-energies leads to small discrepancies in large energy background (muon) spectrum in each crystal



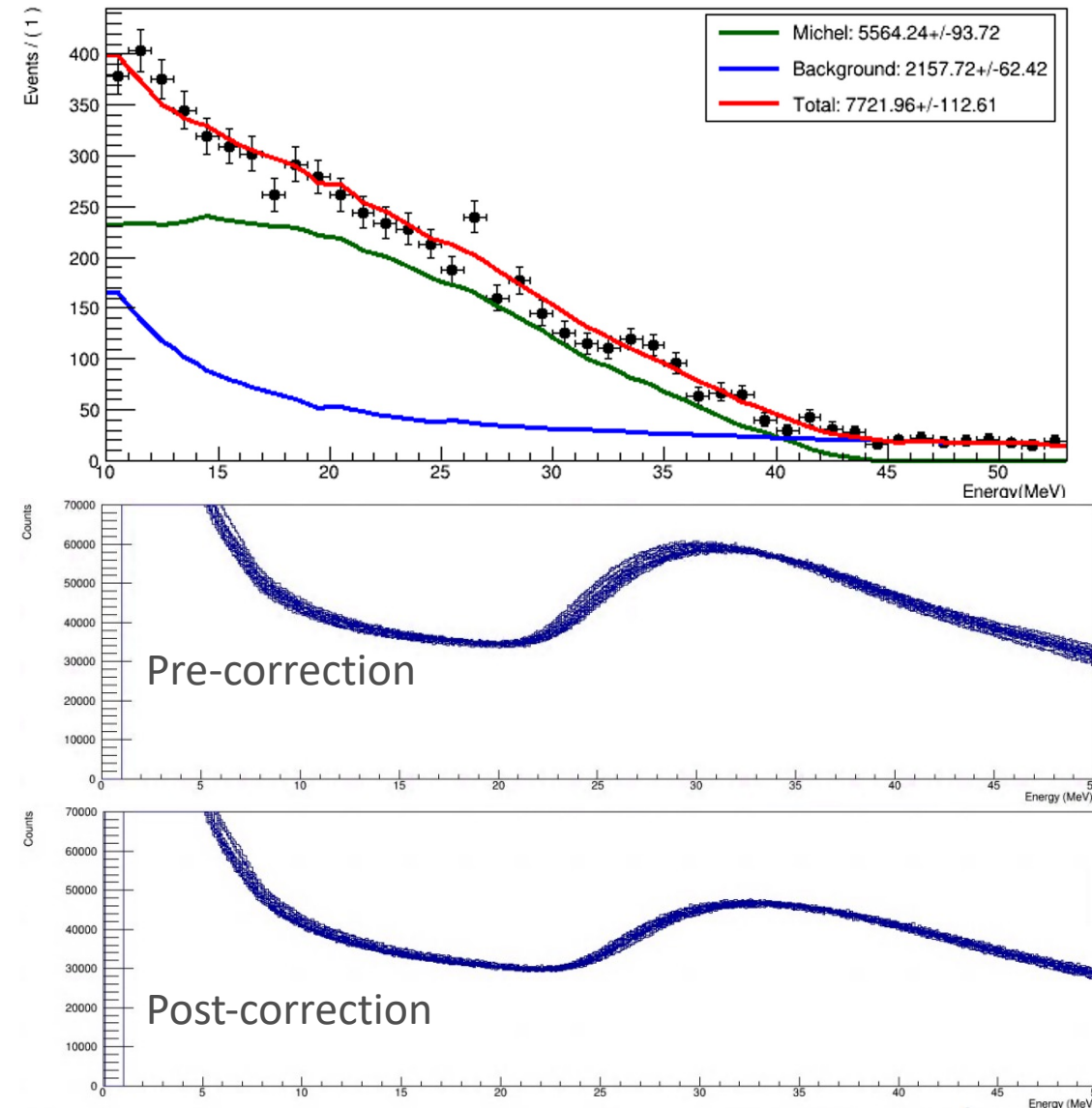
# Michel Positron Correction

- Use Michel positrons to correct calibration
- Collect population of Michel events by looking for large energy depositions in crystals after a muon event (tagged with veto panels)
  - Fitting data gives anti-muon mean lifetime of  $2.172 \pm 0.024\mu\text{s}$
- Simulate positrons in GEANT4, matching data selection criteria
- Fit quadratic calibration function to data that preserves low energy calibrations



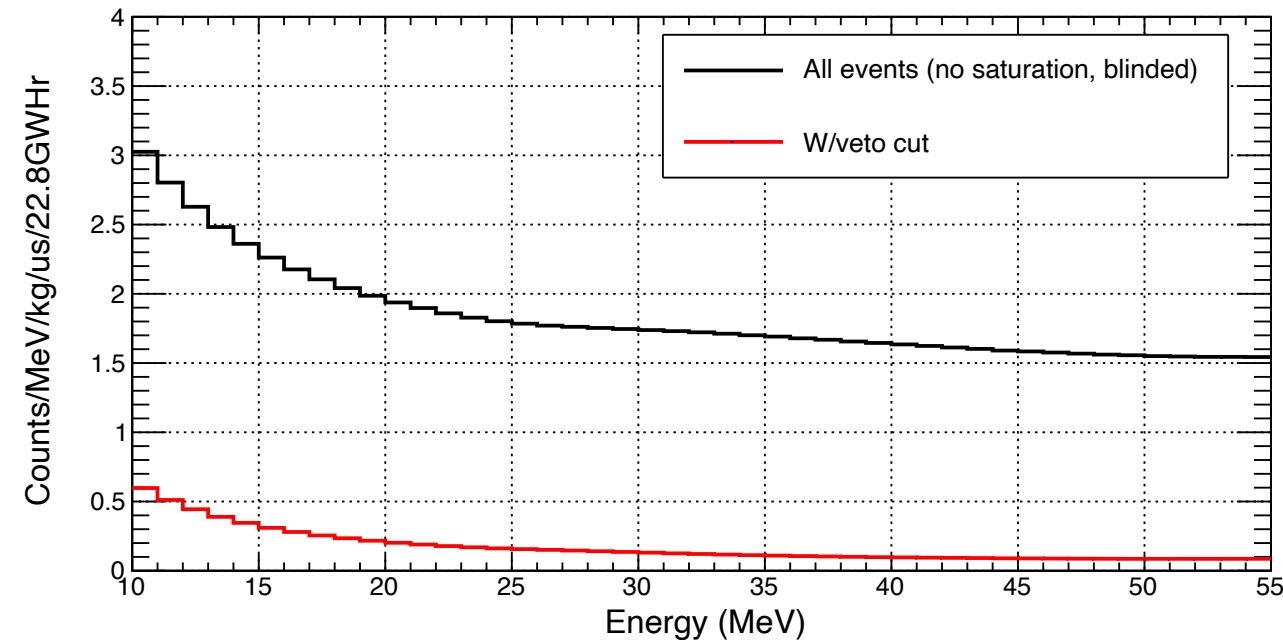
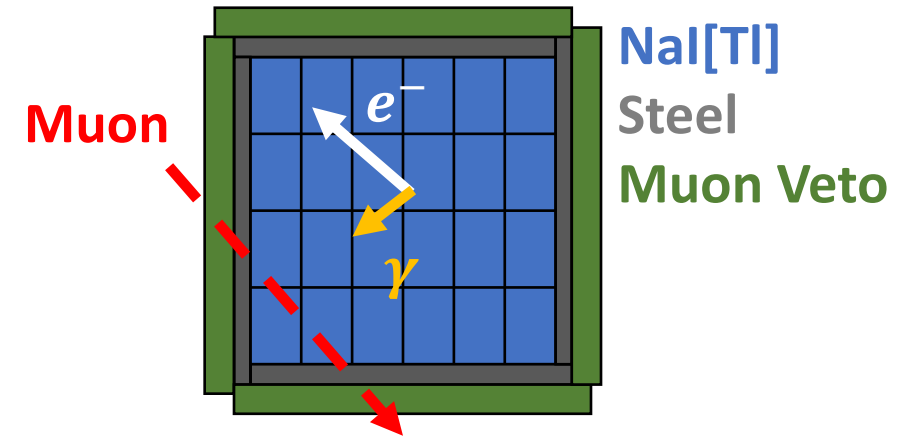
# Michel Positron Correction

- Use Michel positrons to correct calibration
- Collect population of Michel events by looking for large energy depositions in crystals after a muon event (tagged with veto panels)
  - Fitting data gives anti-muon mean lifetime of  $2.172 \pm 0.024\mu\text{s}$
- Simulate positrons in GEANT4, matching data selection criteria
- Fit quadratic calibration function to data that preserves low energy calibrations



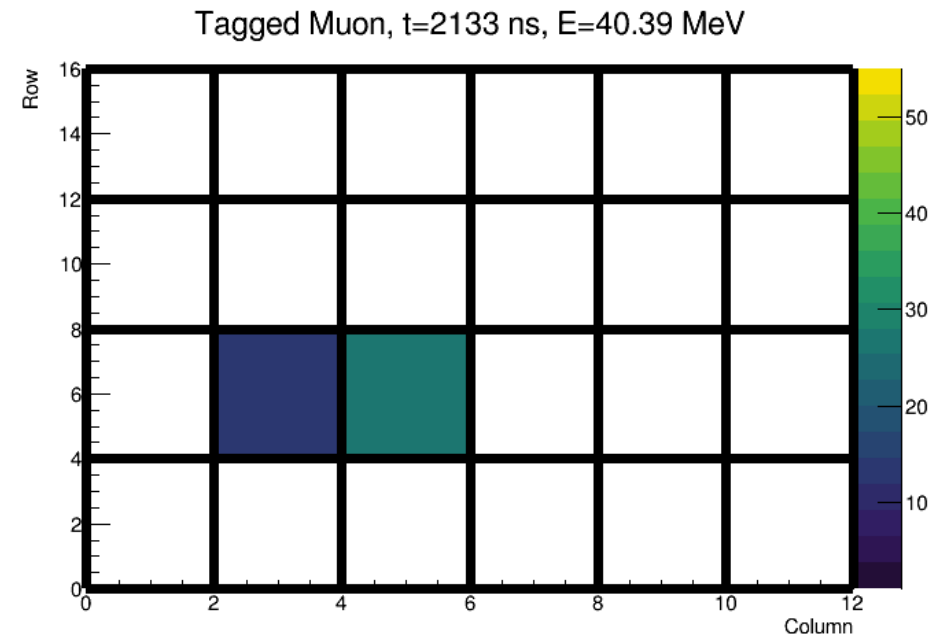
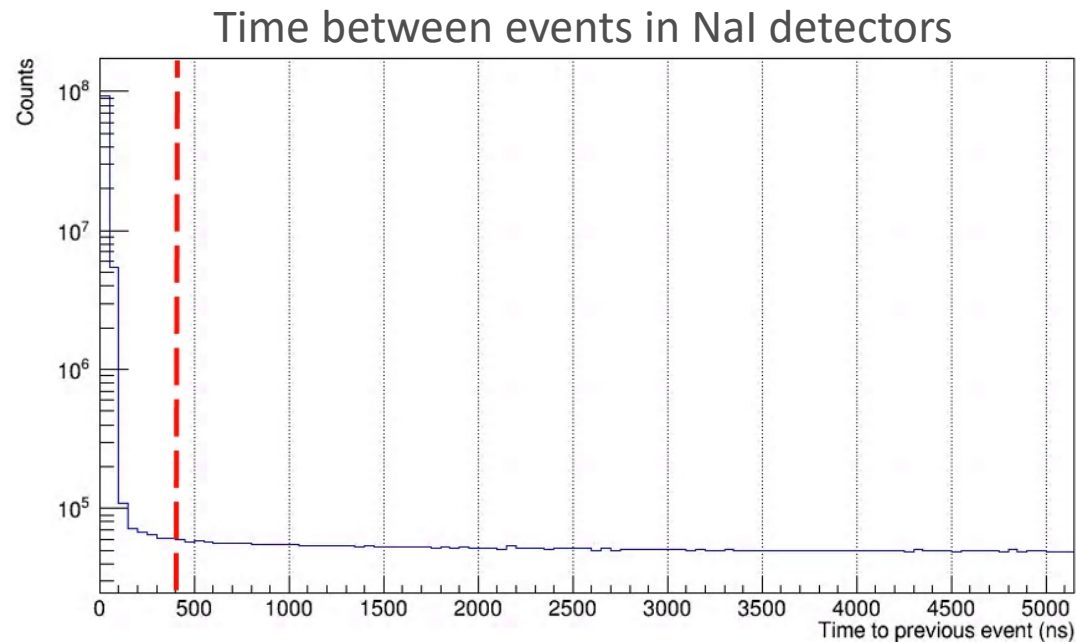
# Muon Veto Cut

- Cosmic muons the largest source of backgrounds for charged-current signal
- Tag NaI events close in time to muon veto panel PMT events above threshold
  - 1.5" steel between NaI crystals and veto panels to avoid vetoing signal
  - Systematic incorporated into analysis to account for uncertainty in veto thresholds
- Veto rejects  $\sim 93\%$  of cosmic muon backgrounds between 10-55 MeV
  - Additionally benefit from looking in a small (several microsecond) window around SNS timing signal to reduce backgrounds



# Event Reconstruction

- Energy from all NaI channels (above 1 MeV threshold) summed together if occur within 400ns window
  - Topology not currently used in analysis, something to study further
- Correlate timing of events with muon veto signals, SNS timing signals





# MARLEY predictions for $^{127}\text{I}$

- MARLEY used for  $^{127}\text{I}$  charged-current predictions along with (p,n) charge-exchange data
- MARLEY's inclusive cross section for DAR neutrinos:

$$22.5_{-6.5}^{+1.2} \times 10^{-40} \text{ cm}^2$$

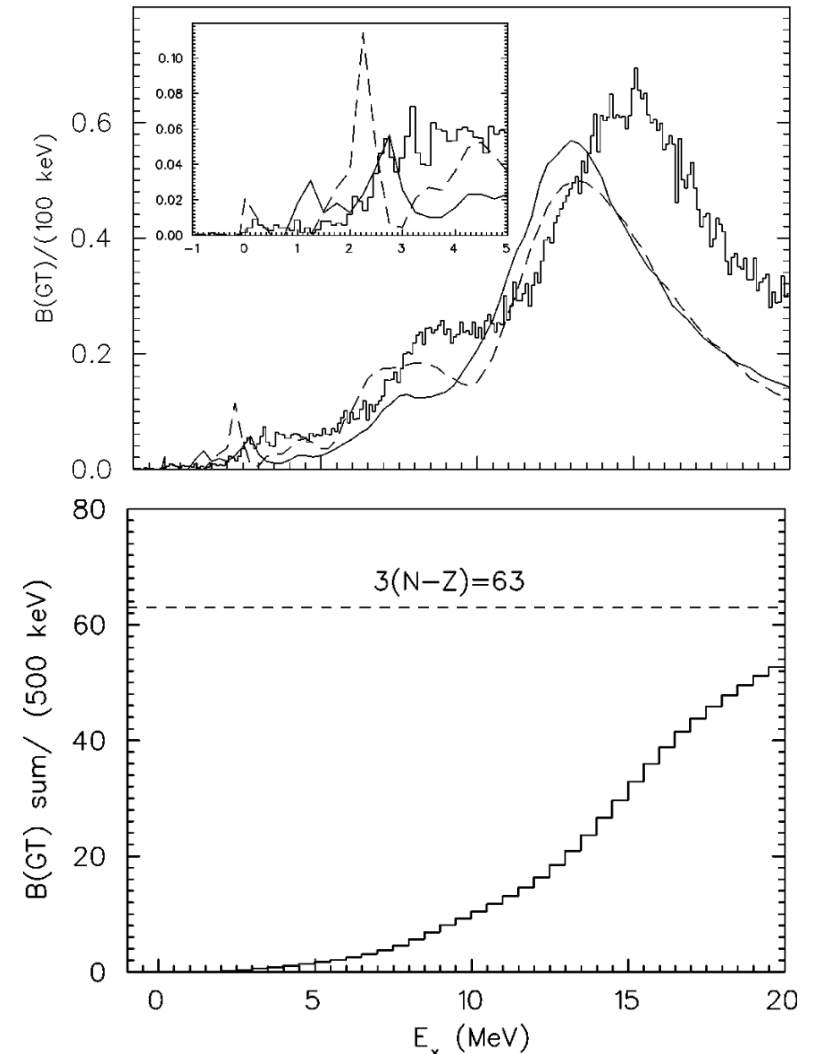
- Uncertainty from  $B(\text{GT}^-)$  normalization uncertainty

- Cross section for exclusive channel to  $^{127}\text{Xe}_{\text{bound}}$ :

$$2.5_{-0.6}^{+0.3} \times 10^{-40} \text{ cm}^2$$

- Good agreement with LAMPF measured value of

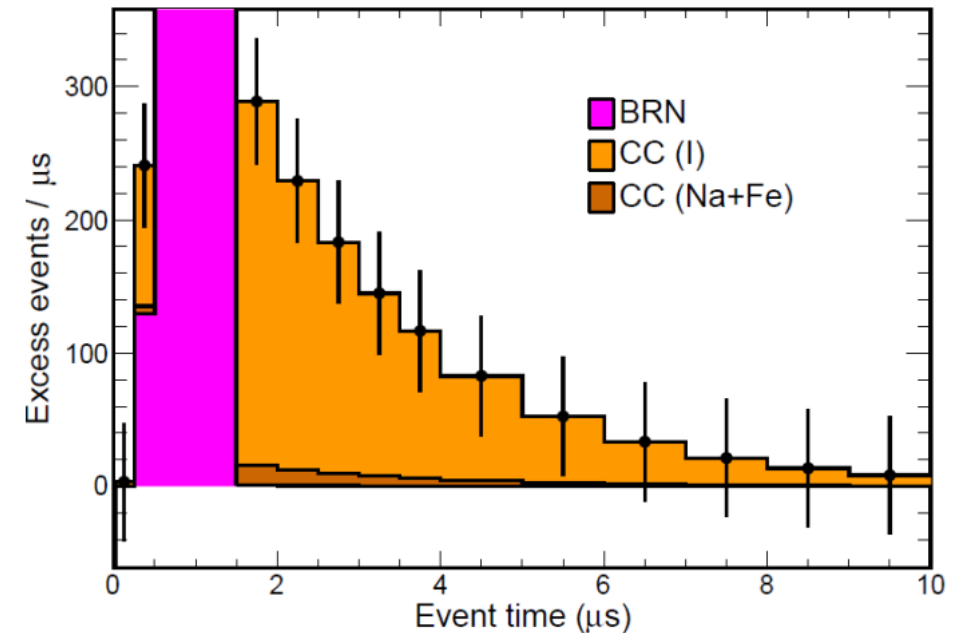
$$2.84 \pm 0.91(\text{stat}) \pm 0.25(\text{sys}) \times 10^{-40} \text{ cm}^2$$



[M. Palarczyk, et al., Phys. Rev. C 59 (1999)]

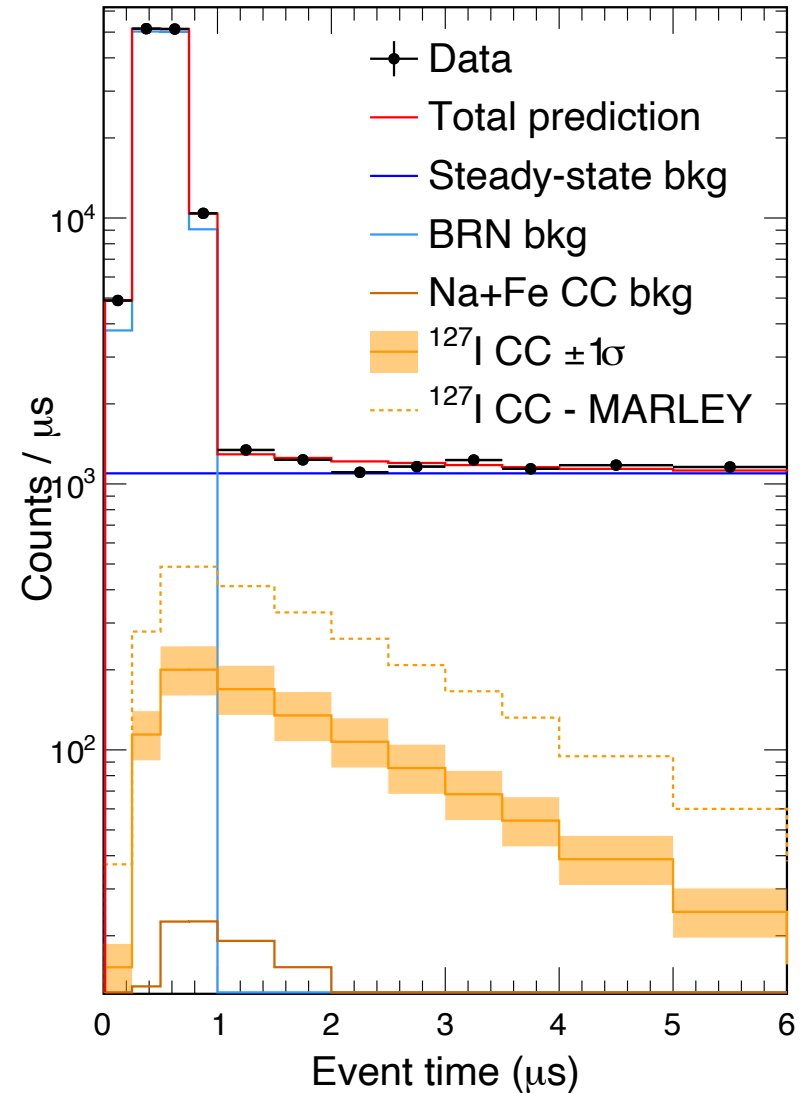
# PDFs

- Simulate charged-current events in GEANT4, process matching analysis cuts to arrive at signal PDF predictions
  - Restrict to 10-55 MeV where most of signal expected to reside, above neutron capture energy on  $^{23}\text{Na}$  and  $^{127}\text{I}$
  - Expect 1,320 CC events on  $^{127}\text{I}$
  - ~61 events from CC on sodium, iron shielding
- Three main results:
  - Inclusive cross-section: 1D fit in time
  - Spectrum of charged-current events: 1D fits in time in 5 MeV energy bins
  - Zero-neutron emission ( $0n$ ) cross section and one-neutron emission ( $1n$ ) cross sections within MARLEY model



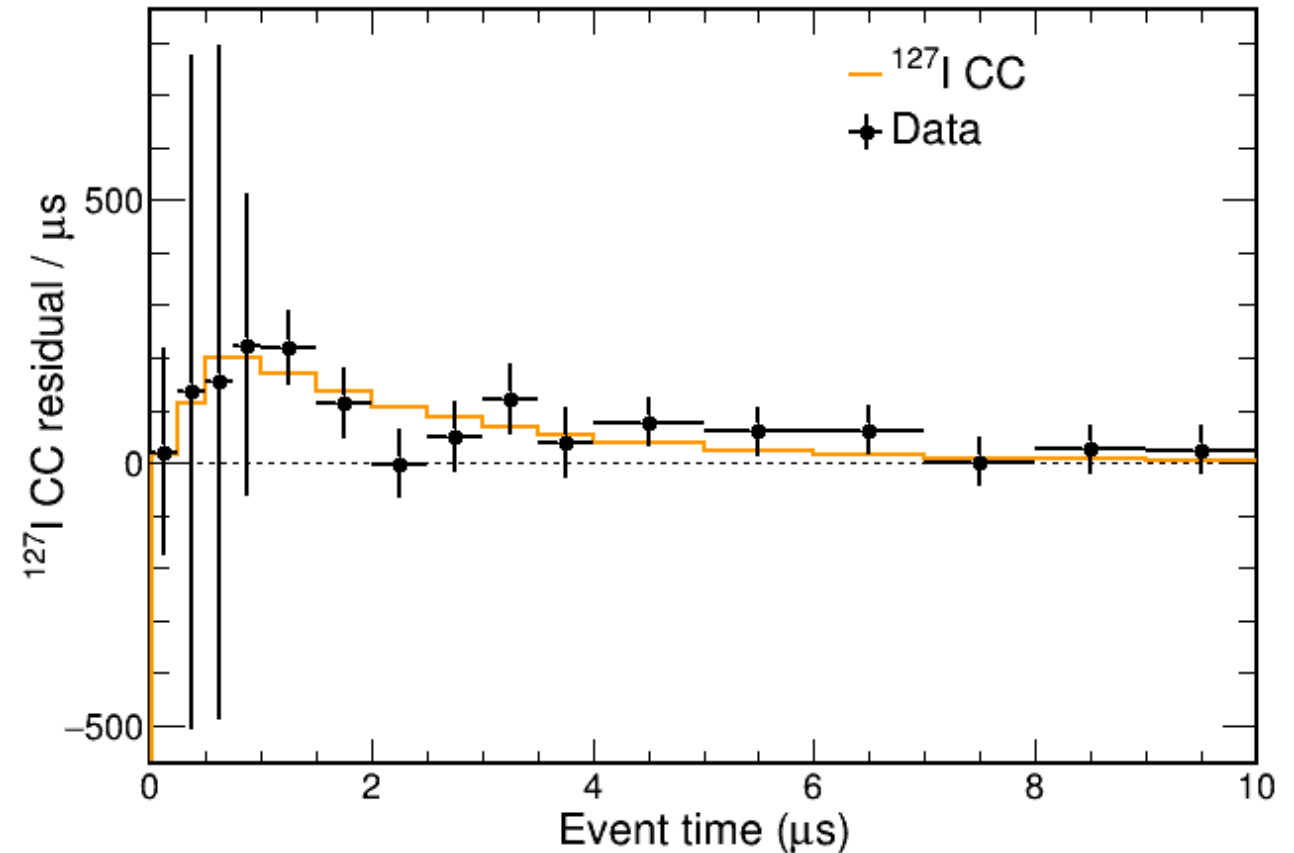
# Results: Inclusive Cross Section

- Best fit gives  $541_{-108}^{+121}$  events
  - $5.8\sigma$  evidence of CC events
  - $\chi^2$  of 13.1, 12 d.o.f.
- Corresponds to cross section of
$$9.2_{-1.8}^{+2.1} \times 10^{-40} \text{ cm}^2$$
  - 40.9% MARLEY cross section



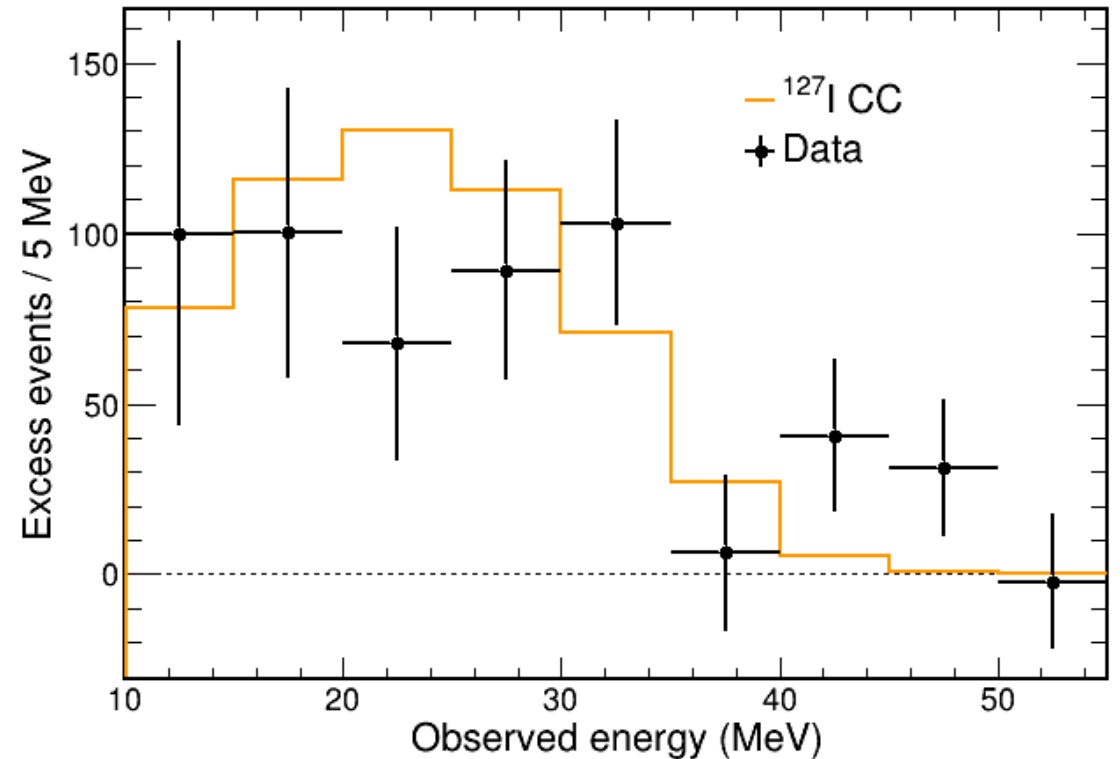
# Results: Inclusive Cross Section

- Best fit gives  $541_{-108}^{+121}$  events
  - $5.8\sigma$  evidence of CC events
  - $\chi^2$  of 13.1, 12 d.o.f.
- Corresponds to cross section of  $9.2_{-1.8}^{+2.1} \times 10^{-40} \text{ cm}^2$ 
  - 40.9% MARLEY cross section
- Subtract off steady-state, BRN backgrounds to form signal residuals for 1D timing fit across 10-55 MeV range



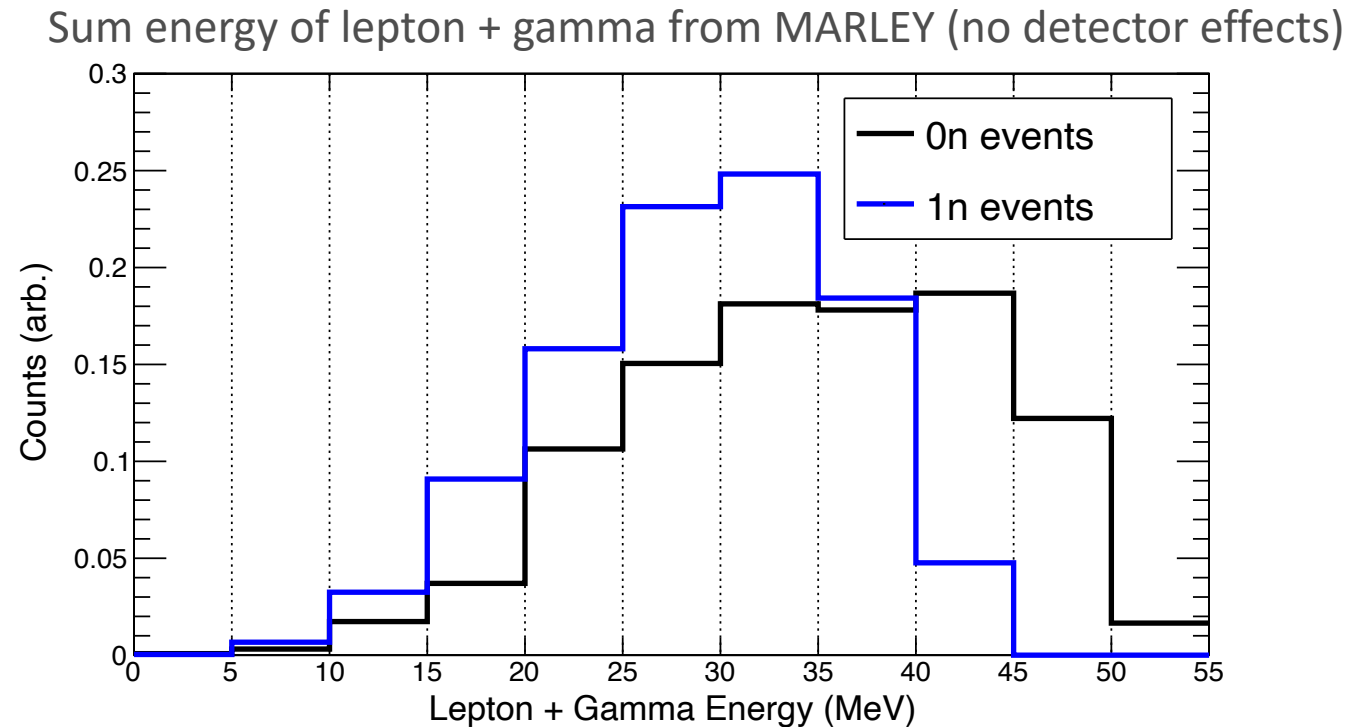
# Results: $^{127}\text{I}$ Charged-Current Spectrum

- Fit 1D timing spectrum in 5 MeV bins from 10-55 MeV to generate an energy spectrum
  - In each bin, independent fits to timing to estimate BRN and CC amplitudes
- Does not show great agreement with scaled MARLEY model, but two caveats
  - Large error bars on due to low statistics
  - Forbidden transitions not incorporated in MARLEY predictions



# Result: $0n/1n$ Cross Sections

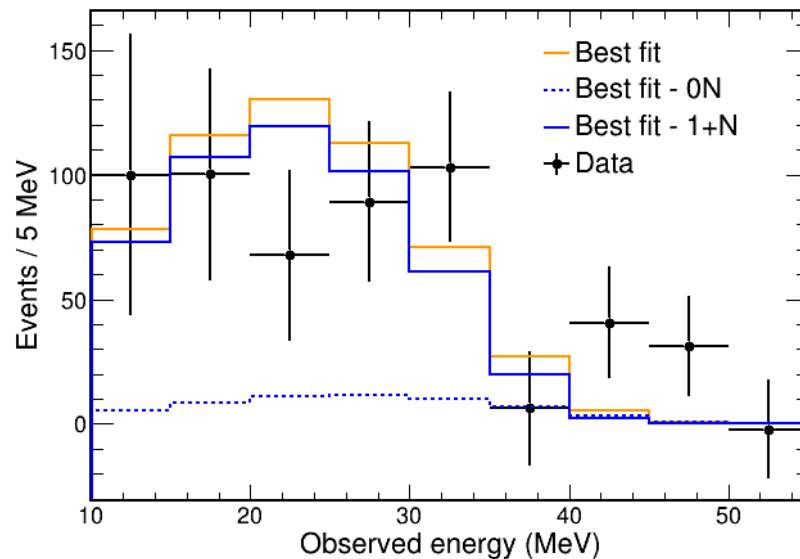
- Different spectrum of visible energy (gammas + lepton) for events with neutron emission ( $1n$ ) compared to those without ( $0n$ )
  - Threshold for  $1n$  emission events is 7.9 MeV compared to  $0n$  threshold of 0.7 MeV
  - Plot intended to demonstrate difference in spectral shape, amplitudes arbitrary



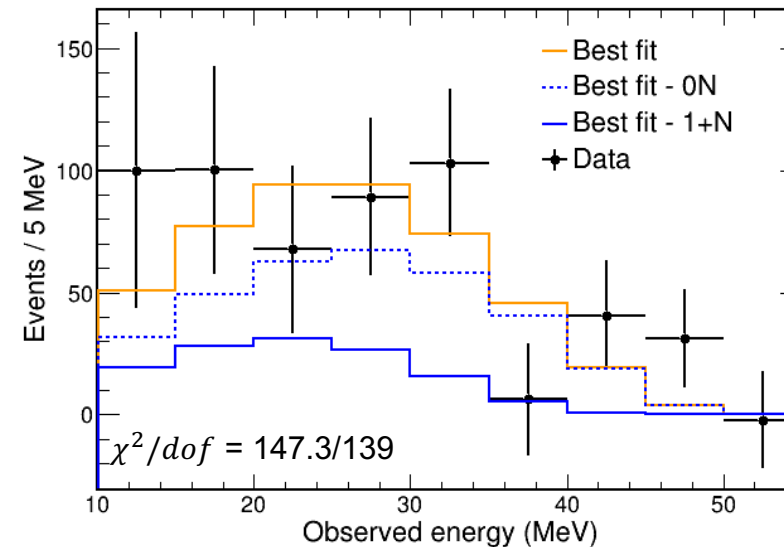
# Result: $0n/1n$ Cross Sections

- After simulating events in detector geometry, allowing  $0n$  and  $1n$  amplitudes to float
- MARLEY predicts 10.6% events are  $0n$ , data favors larger fraction (72.3%) of events are  $0n$
- $0n$  cross section:  $5.2_{-3.1}^{+3.4} \times 10^{-40} \text{cm}^2$ 
  - Compare to LAMPF measured value:  $2.84 \pm 0.91(\text{stat}) \pm 0.25(\text{sys}) \times 10^{-40} \text{cm}^2$
- $1n$  cross section:  $2.4_{-2.4}^{+3.3} \times 10^{-40} \text{cm}^2$

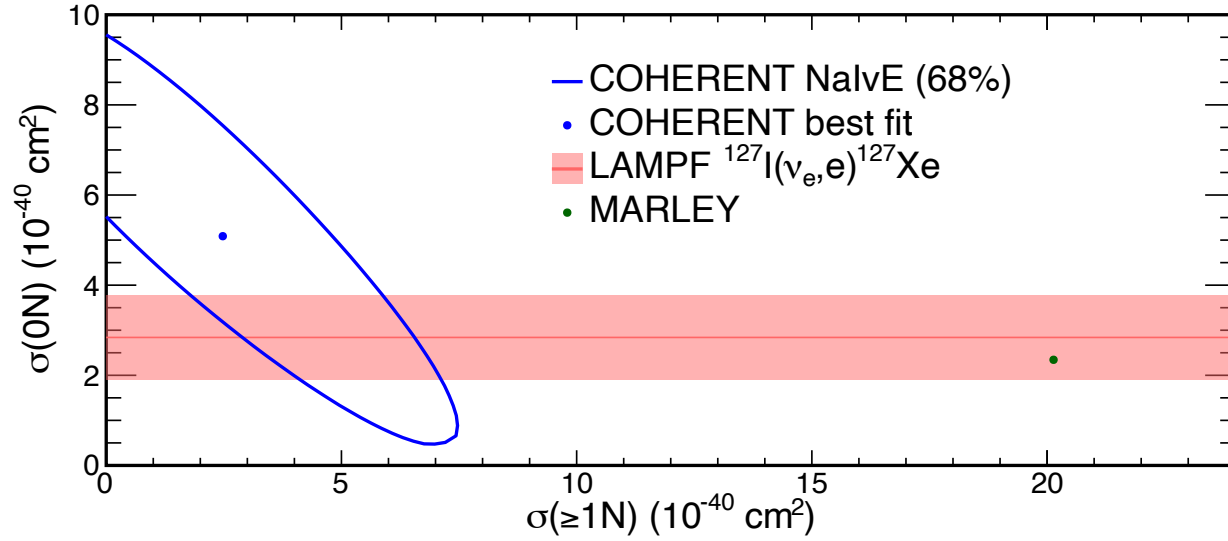
Nominal MARLEY prediction: 10.6%  $0n$  events



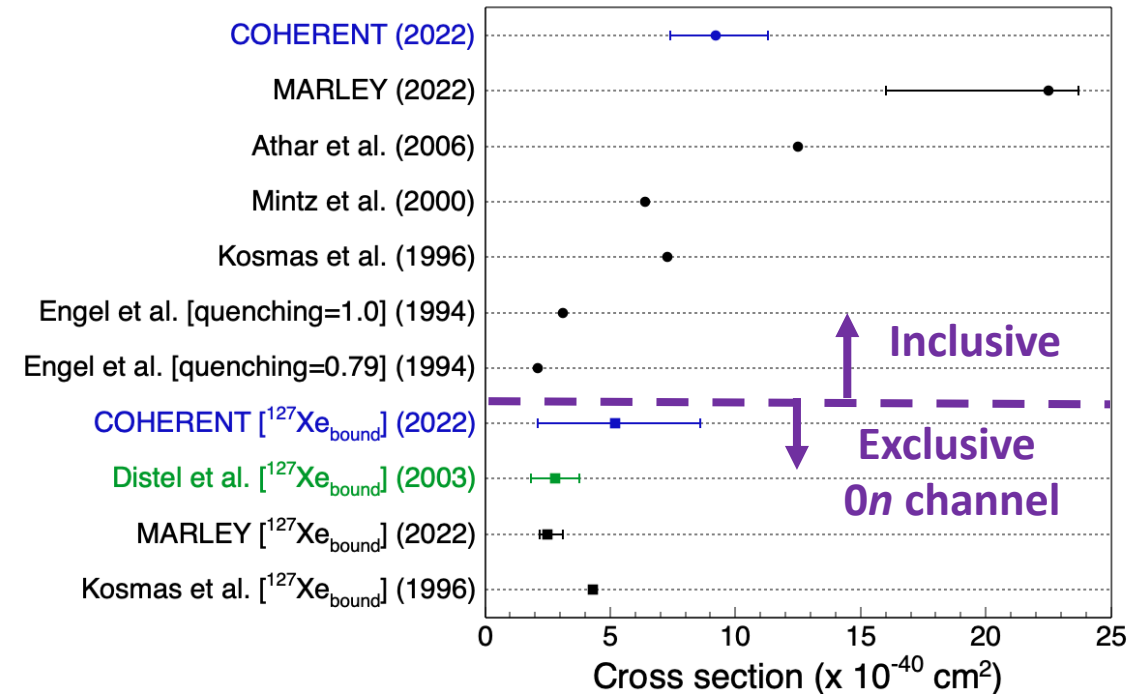
Best fit value: 72.3%  $0n$  events



# Comparison of Results



$^{127}\text{I}$  Flux-Averaged DAR Cross Sections

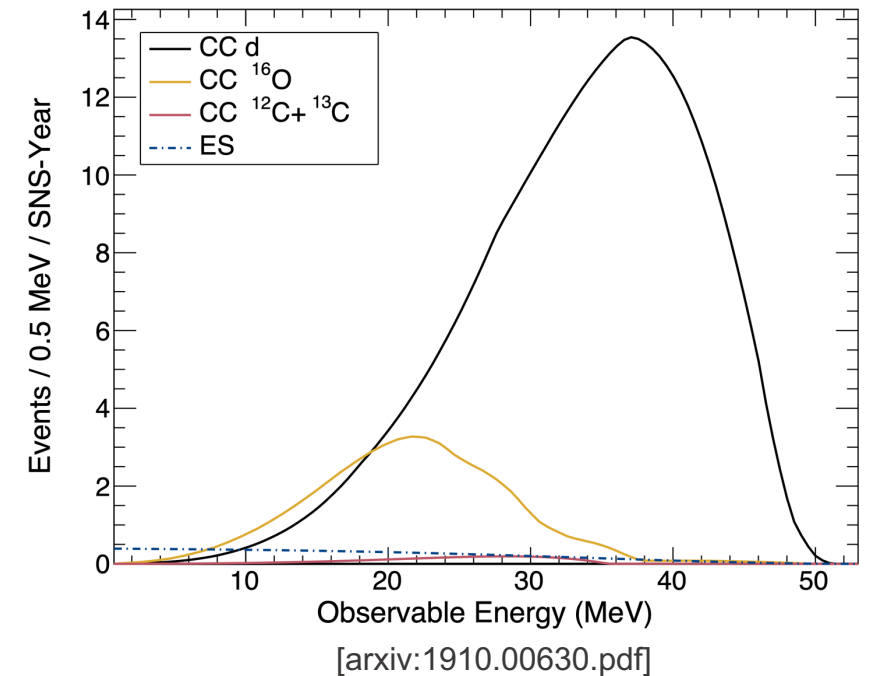




# COHERENT's Future Inelastic Neutrino-Nucleus Measurements

# D<sub>2</sub>O for Flux Normalization

- Neutrino flux one of largest uncertainties at SNS,  $\sim 10\%$ 
  - $\nu_e$  CC cross section on  $^2\text{H}$  calculated to within 2-3%
- Deploying 600-kg D<sub>2</sub>O detector measure flux, reduce uncertainties
- May also be able to measure  $^{16}\text{O}$  charged-current events
  - Potentially useful for understanding supernova neutrinos interacting via this channel in large water detectors



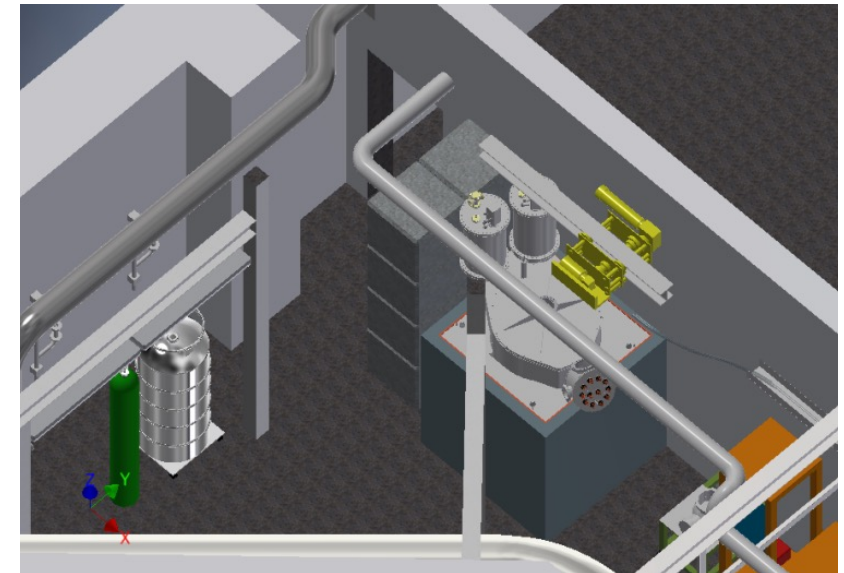
# CENNS-10/CENNS-750

- CENNS-10 single-phase liquid argon detector with 24-kg fiducial volume, deployed in 2016
  - Primary goal to measure CEvNS, data being studied to see what can be said about inelastic events on  $^{40}\text{Ar}$
- CENNS-750 upgrade in development, increase statistics and go after charged-current interactions on  $^{40}\text{Ar}$ 
  - Recent funding from Korea National Research Foundation (Jun 1, 2022)
  - Will study CEvNS, charged-current, and dark matter

CENNS-10:

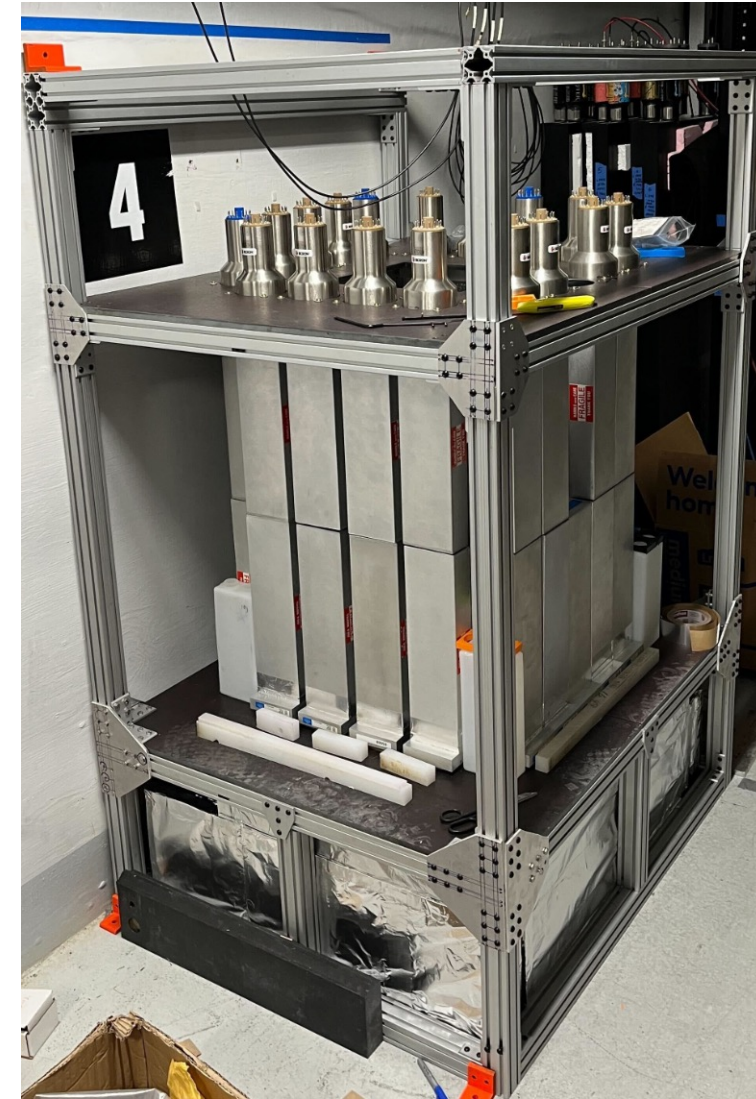


CENNS-750:



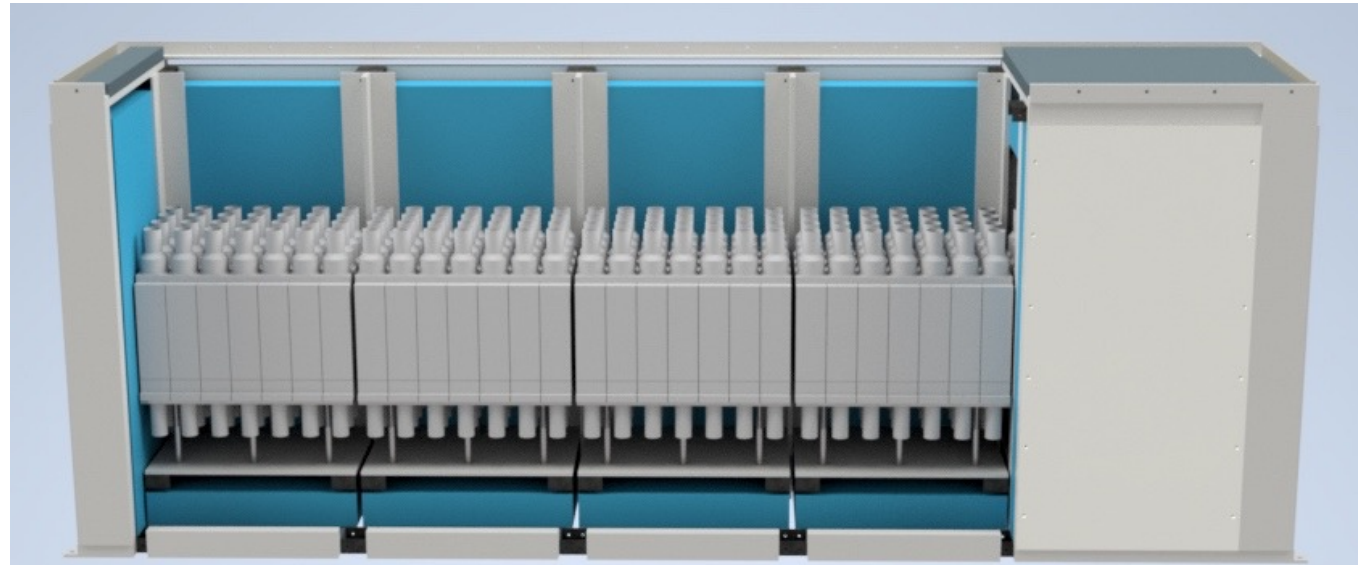
# NuThor: Neutrino-Induced Fission

- Detector designed to study neutrino-induced fission, a long-theorized but never observed process
- Looks for neutrons from neutrino-induced fission through capture of gadolinium-doped water
- Initial data collection has started!



# NalvETe

- NaI neutrino Experiment TonnE-scale (**NalvETe**)
- Ton-scale version of NalvE-185, consisting of 315 NaI detectors (2,425 kg)
- Main goal is to measure CEvNS on  $^{23}\text{Na}$
- Space left in design to implement muon veto panel to enable charged-current measurement
- Better gamma shielding, water shielding, and improved statistics from larger mass, may be able to go after CC on  $^{23}\text{Na}/^{27}\text{Al}$  as well



# Summary

- COHERENT has results from its first searches for inelastic neutrino-nucleus scattering at the SNS
  - Lead neutrino cube reports NIN cross section on lead suppressed by factor  $0.29_{-0.17}^{+0.17}$  compared with MARLEY model
  - NalvE-185 reports cross section 40.9% lower than predicted
  - Shows need for improved understanding of uncertainties in nuclear models
- More analysis to be done on existing datasets:
  - $2n$  emission events for lead neutrino cube
  - NIN analysis for iron neutrino cube
  - Machine learning approach for NalvE-185
- Suite of other detectors coming online in the next few years, should expand existing low-energy inelastic neutrino-nucleus measurements
  - D<sub>2</sub>O for reducing flux uncertainty, <sup>16</sup>O CC events
  - NuThor for neutrino-induced fission on <sup>232</sup>Th
  - NalvETe increase stats on <sup>127</sup>I CC, potentially <sup>23</sup>Na/<sup>27</sup>Al CC as well
  - CENNS-750 for <sup>40</sup>Ar

# Acknowledgements

- Thanks to **Brandon Becker** (GEANT4 lead neutrino cube simulations), **Peibo An** (NalvE simulations/Michel calibration), **Daniel Pershey** (lead neutrino cube/NalvE fitting)
- This work was performed under the auspices of the U.S. Department of Energy by Lawrence Livermore National Laboratory under Contract DE-AC52-07NA27344.



U.S. DEPARTMENT OF  
**ENERGY**

Office of  
Science



한국연구재단  
National Research Foundation of Korea

**NNSA**  
National Nuclear Security Administration



Thank you for your attention!

# Back-up



# NaIvE Uncertainties

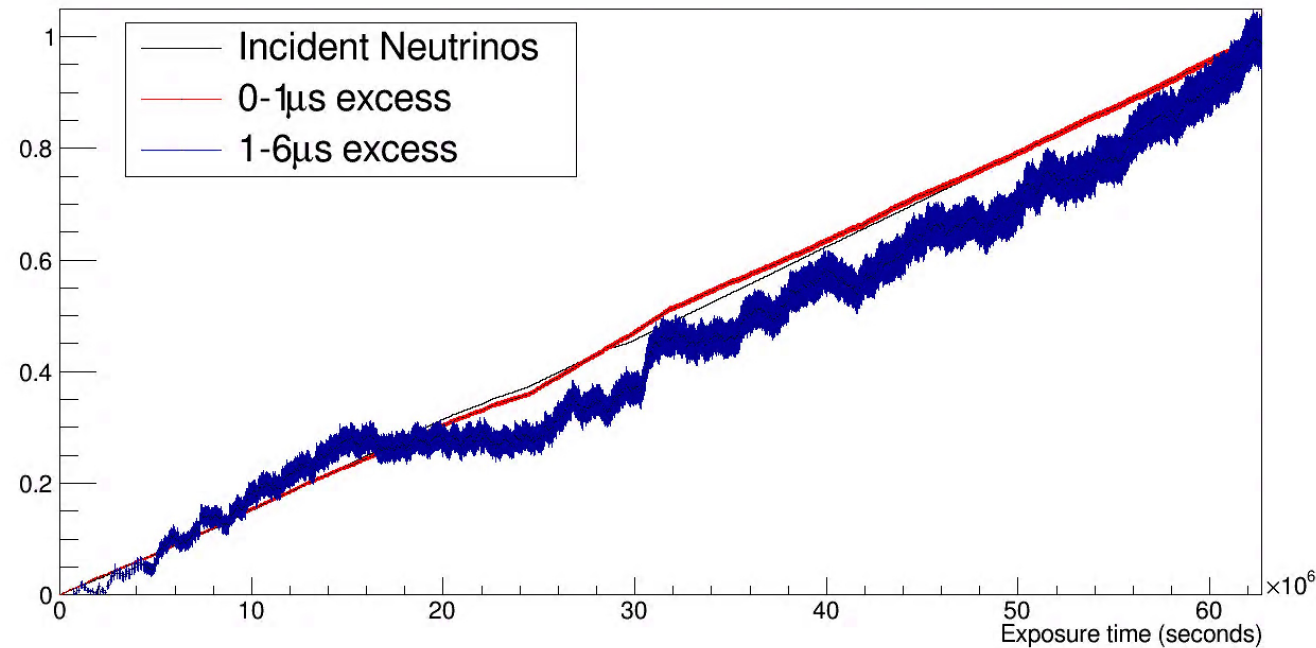
- Largest uncertainty is neutrino flux (again!)
- Second largest uncertainty is due to unknown veto threshold, non-uniformity of light collection from muon veto panels
  - Even with 1.5” steel between NaI detector and veto panels, some charged-current signal triggers veto system in simulation
- Signal mostly at higher energies, uncertainties in calibration, energy resolution, trigger efficiency have little effect on number of counts in energy region-of-interest

Quantity	I-CC Unc [%]	Na-CC Unc [%]	Fe-CC Unc [%]
Neutrino flux	±10.0	±10.0	±10.0
Trigger Efficiency	+0.0 -0.3	+0.0 -0.1	+0.0 -1.0
Calibration	+0.0 -0.0	+0.0 -0.0	+0.1 -0.3
Energy Resolution	+0.0 -0.0	+0.0 -0.0	+0.2 -0.2
Muon Veto Threshold	+2.8 -5.1	+1.1 -2.0	+2.0 -3.7
<b>Total:</b>	+10.4 -11.2	+10.1 -10.2	+10.2 -10.7

Event Type	nTargets ( $\times 10^{26}$ )	MARLEY $\sigma$ ( $\times 10^{-40} \text{cm}^2$ )	Eff.	Unc.	Number
I-CC	7.4	22.5	0.758	+10.4-11.2	1320 <sup>+148</sup> <sub>-137</sub>
Na-CC	7.4	0.5	0.793	+10.1-10.2	31 <sup>+3</sup> <sub>-3</sub>
Fe-CC	50.0	2.9	0.021	+10.2-10.7	31 <sup>+3</sup> <sub>-3</sub>

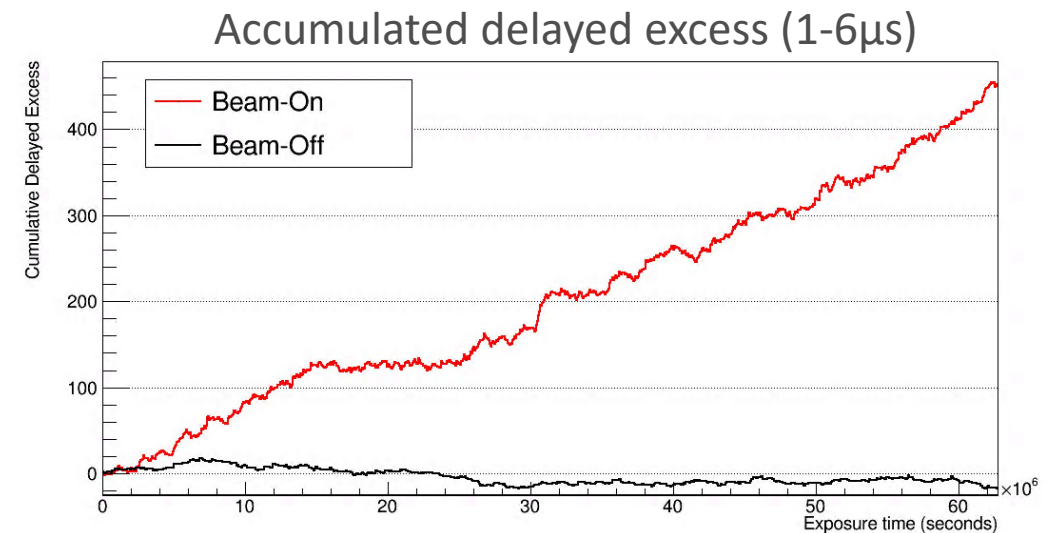
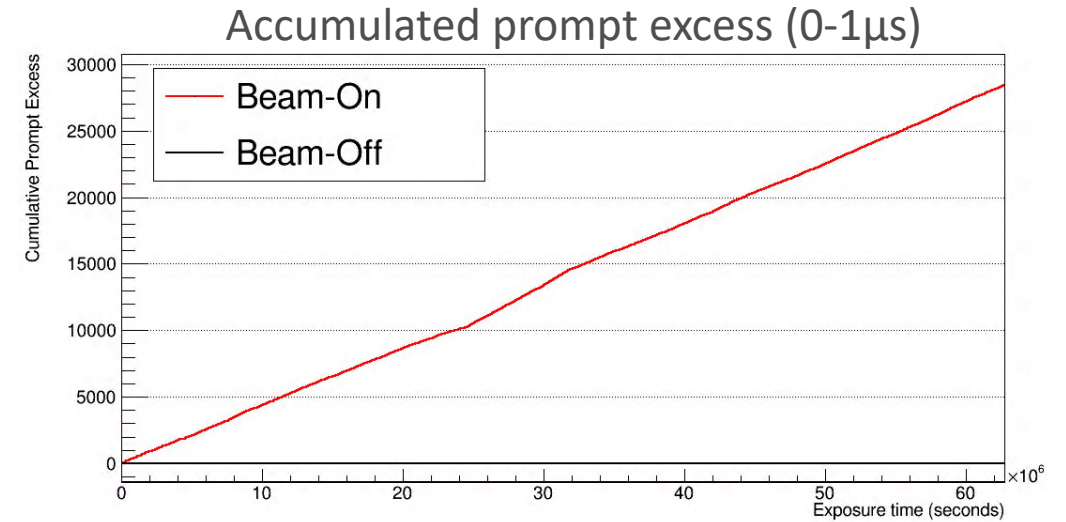
# Post-Unblinding Checks

- K-S test shows good agreement between prompt and delayed excesses and delivered beam
  - With 1000 pseudo-experiments, K-S probabilities are 1.000 and 0.987 from prompt and delayed excesses



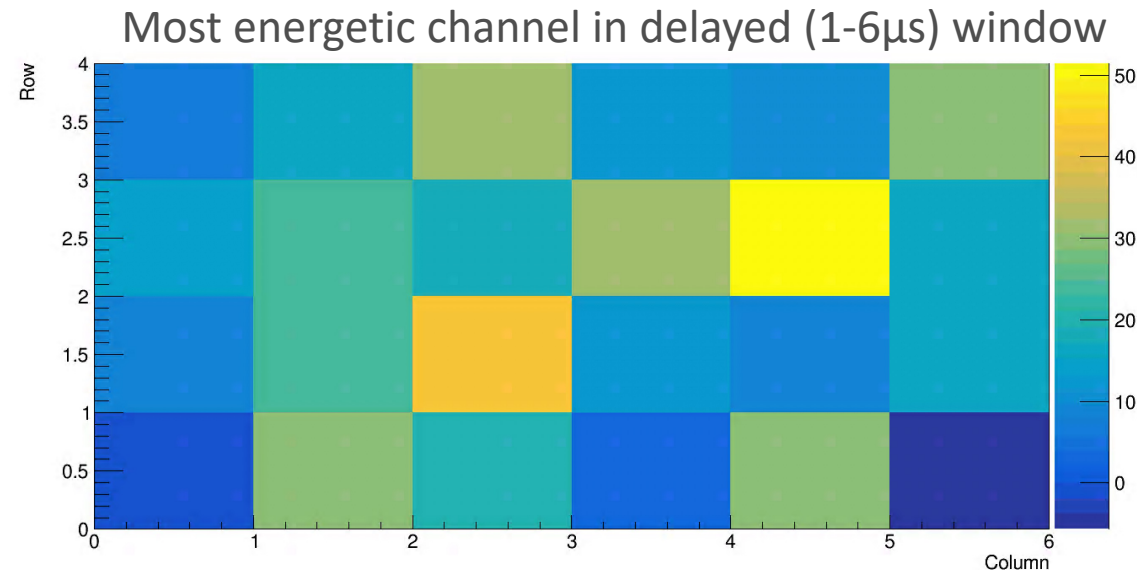
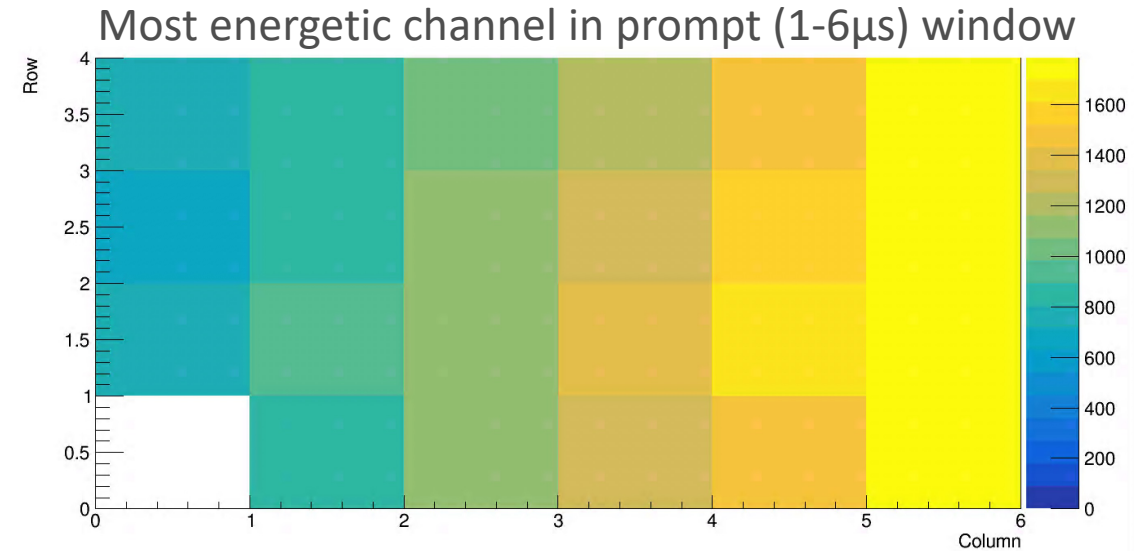
# Post-Unblinding Checks

- K-S test shows good agreement between prompt and delayed excesses and delivered beam
  - With 1000 pseudo-experiments, K-S probabilities are 1.000 and 0.987 from prompt and delayed excesses
- No excess observed in prompt/delayed windows when beam not on target



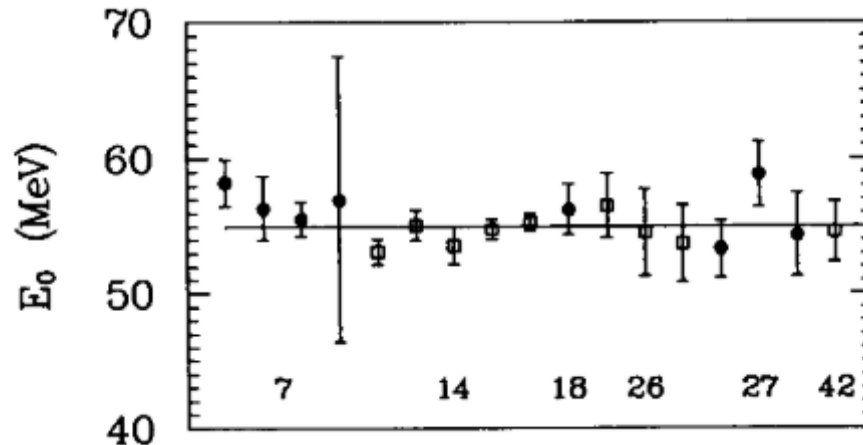
# Post-Unblinding Checks

- K-S test shows good agreement between prompt and delayed excesses and delivered beam
  - With 1000 pseudo-experiments, K-S probabilities are 1.000 and 0.987 from prompt and delayed excesses
- No excess observed in prompt/delayed windows when beam not on target
- Some initial topology studies show neutrons incident on detector from side, do not see same pattern for delayed events
  - Helps understand BRN background for COHERENT's other detectors



# NaIvE: $g_A$ quenching

- Definition of matrix elements in (p,n) and weak interactions differs by  $g_A^2$
- Cannot determine the value of  $g_A$  from cross section
  - Forbidden transitions not included in MARLEY
- Can set limit on maximum value of  $g_A$ , with large caveat:
  - Normalization for B(GT) in (p,n) charge-exchange measurements assumes a value for  $g_A=1.26$ , compares  $0^\circ$  scattering cross sections with beta-decay half-lives
  - Heaviest element used in normalization has  $A=42$
  - Incorrect normalization for strengths in (p,n) experiments would lead to incorrect value of  $g_A$



[T. Taddeucci, et al., Nuc. Phys. A 469 (1987)]

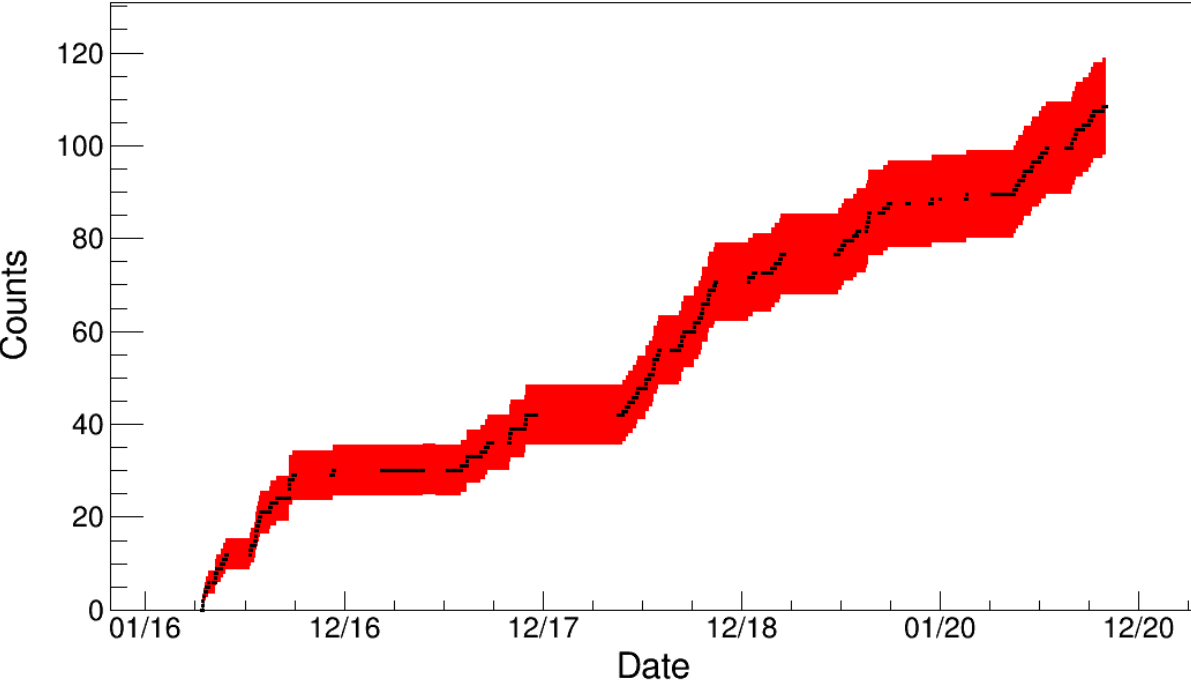
# Lead NIN Uncertainties

- Largest source of uncertainty (10%) due to uncertainty in neutrino flux
  - D<sub>2</sub>O detector being deployed to SNS to measure flux via the electron neutrino charged-current cross section on <sup>2</sup>H
  - 2-3% theoretical uncertainty
- Second largest uncertainty due to quenching factor of nuclear recoils in EJ-301 liquid scintillator
  - Members of collaboration measured this at low recoil energies at TUNL

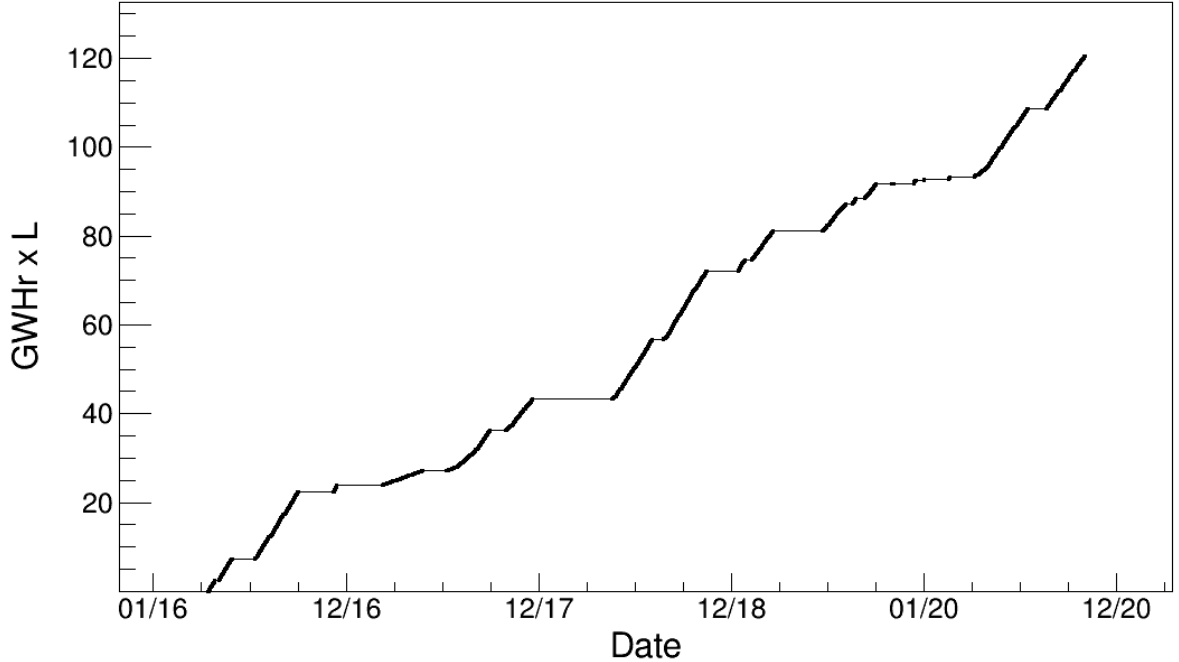
Source	NIN uncertainty (%)
Neutrino flux	$\pm 10$
Quenching factor	$\pm 2.7$
Software threshold	+0.2 / -0.4
PSD selection	$\pm 1.0$
Calibration	+2.1 / -2.2
Energy resolution	+1.7 / -0.5
Muon veto	+0.4 / -0.3
Lead target mass	$\pm 0.6$
MARLEY NC prediction	+0 / -1.6
Total:	+10.8 / -10.8

# Lead Neutrino Cube: Prompt Signal vs. Beam Power

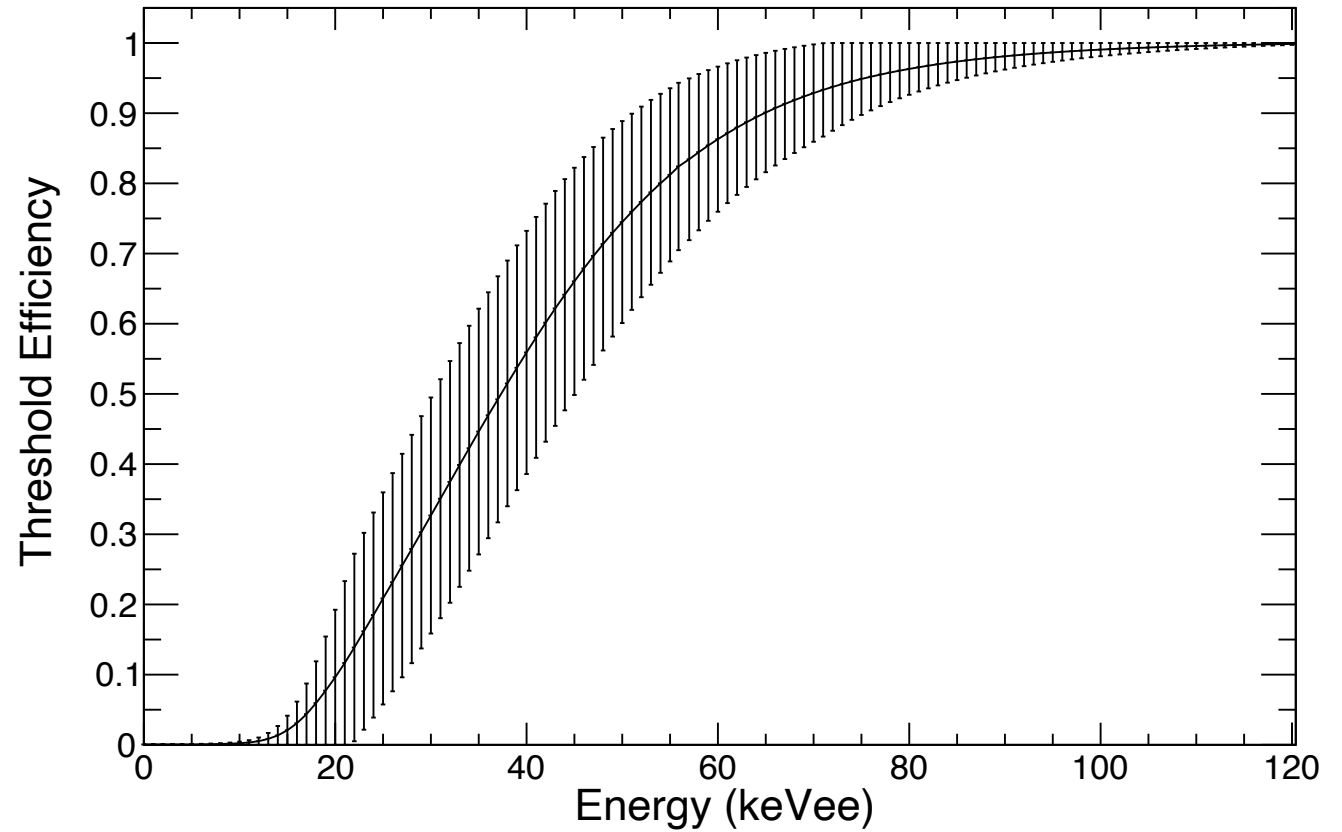
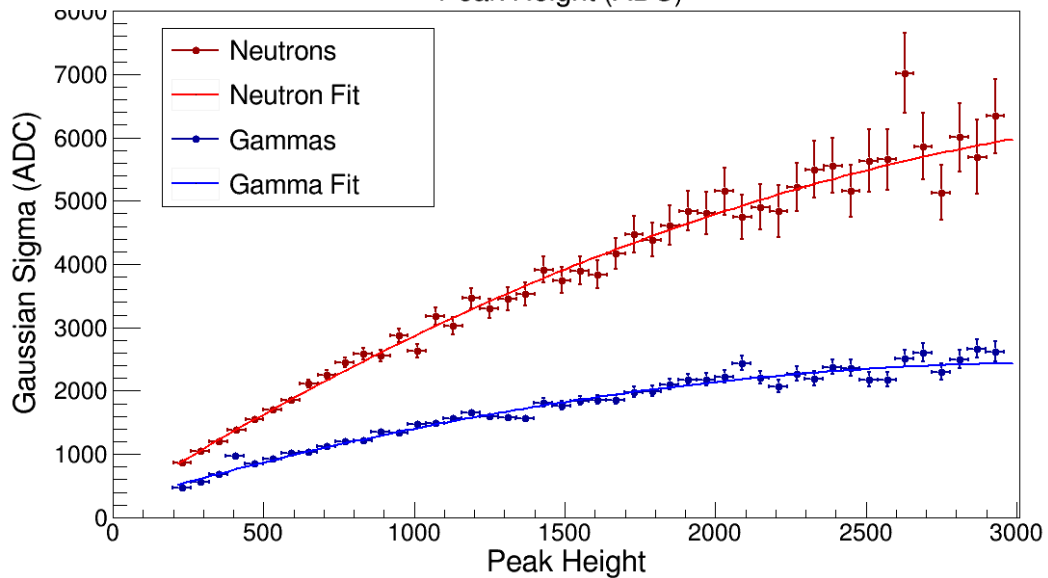
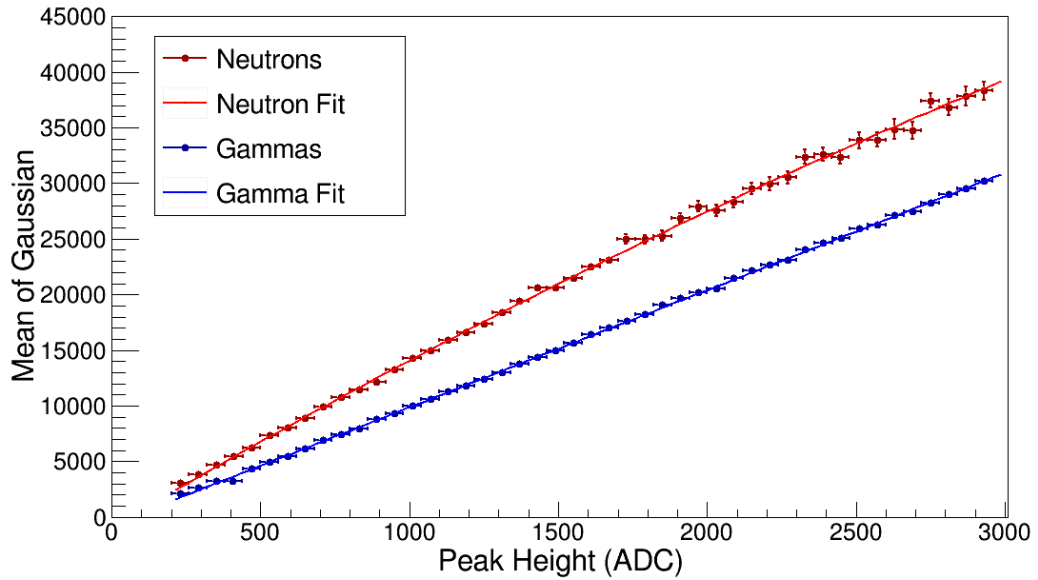
Prompt signal excess (BRNs)



Delivered beam power



# Lead Neutrino Cube: Trigger Thresholds





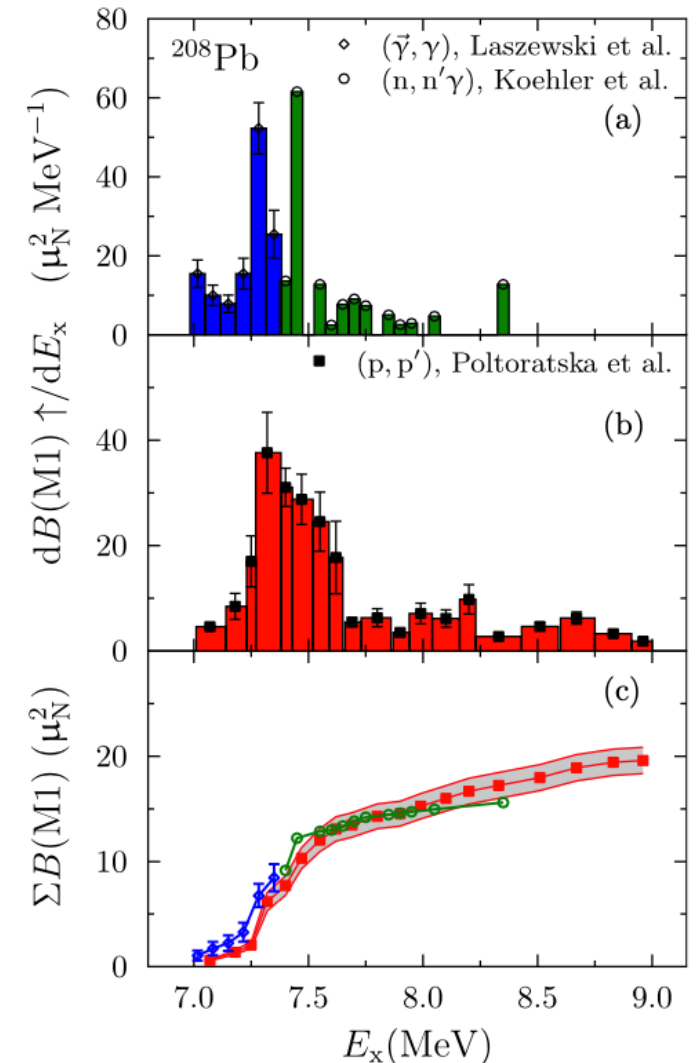
# Lead Neutrino Cube: Neutral-Current Predictions

- MARLEY can generate NC predictions using  $B(GT_0)$  data
  - Input is  $B(M1)$  data along with approximate conversion from  $B(M1)$  to  $B(GT_0)$  from S. V. Semenov, Bull. of the Rus. Acad. of Sci.: Physics **81**, (2017)

$$B(GT_0) = \frac{4\pi g_A^2}{3\mu_\nu^2} \frac{B(M1)}{\mu_N^2}$$

- Cross section significantly smaller than CC prediction, will increase w/forbidden transitions

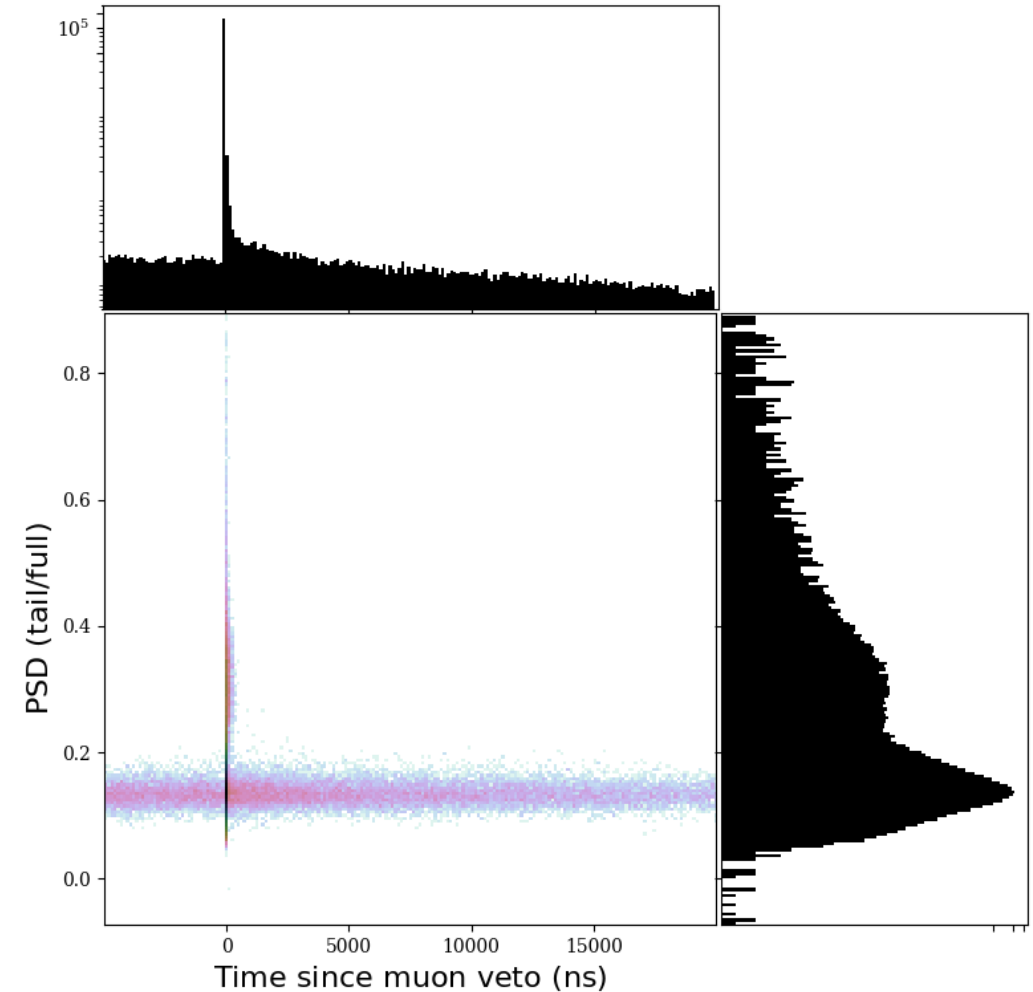
Reaction Channel	$\bar{\sigma} (\times 10^{-40} \text{cm}^2)$	Notes	Reference
$^{208}\text{Pb}(\nu_x, \nu'_x)\text{X}$	4.09	$\nu_e$	Suzuki, et al. (2003) [160]
	2.087	$\nu_e$ and $\bar{\nu}_\mu$	S. V. Semenov (2017) [127]
	0.68	$\nu_e$	MARLEY, $B(GT_0)$ from [128, 166]
	0.48	$\nu_\mu$	MARLEY, $B(GT_0)$ from [128, 166]
	0.97	$\bar{\nu}_\mu$	MARLEY, $B(GT_0)$ from [128, 166]
$^{208}\text{Pb}(\nu_x, \nu'_x n)^{207}\text{Pb}$	0.46	$\nu_e$	MARLEY, $B(GT_0)$ from [128, 166]
	0.33	$\nu_\mu$	MARLEY, $B(GT_0)$ from [128, 166]
	0.65	$\bar{\nu}_\mu$	MARLEY, $B(GT_0)$ from [128, 166]



[I. Poltoratska, et al., Phys. Rev. C **93**, 041302(R) (2016)]

# Lead Neutrino Cube: Muon Veto Cut

- Establish events with 2+ muon veto PMTs within 250ns period a veto event
  - Requirement for 2+ PMTs reduces dead time due to background radiation, fluctuations in PMT rates
- Plot the time, energy of liquid scintillator events near muon veto events (occur at  $t=0$  in plot)
- See large population of muon-induced neutrons shortly after muon
- Final cut is  $[-200\text{ns}, +25,000\text{ns}]$  following a 2+ PMT veto event



# Lead Neutrino Cube: PSD Fitting

Ch0 fit from 100 to 125 keV

